This is to certify that the
thesis entitled

FORENSIC ANALYSIS OF COSMETIC FACE POWDERS

presented by

KELLY GREENOUGH

has been accepted towards fulfillment
of the requirements for the

M.S. degree in Forensic Science

L. A. Waddell
Major Professor's Signature

4/27/07
Date

FORENSIC ANALYSIS OF COSMETIC FACE POWDERS

By

Kelly Greenough

A THESIS

Submitted to
Michigan State University
in partial fulfillment of the requirements
for the degree of

MASTER OF SCIENCE

Department of Criminal Justice

2007

ABSTRACT

FORENSIC ANALYSIS OF COSMETIC FACE POWDERS

By

Kelly Greenough

Cosmetic face powders are widely used and a large amount is applied to the facial region, thus making it possible to be transferred during the course of a crime. Therefore, powders have potential to be used as forensic evidence. In such a case, it may be useful to determine if two powder samples originated from a common source. The purpose of this project is to determine if various samples of cosmetic face powder can be differentiated from one another.

In this work, three analytical techniques were selected to differentiate between pairs of cosmetic face powder samples. The chosen techniques included scanning electron microscopy-energy dispersive spectroscopy (SEM-EDS), attenuated total reflectance-Fourier transform infrared spectroscopy (ATR-FTIR), and matrix-assisted laser desorption ionization mass spectrometry (MALDI-MS). Each method analyzes different components of the face powders, and the data are thus complementary.

Twenty-seven samples were analyzed in this project, and each of the possible pairs of samples was compared in order to evaluate the discrimination ability of each technique. The individual techniques and the combined techniques achieve a high level of discrimination between face powder samples, displaying the usefulness of cosmetic face powders in forensic investigations.

ACKNOWLEDGEMENTS

I would like to thank several people for their help and support during the time this project was taking place. First, I would like to thank my advisor, Dr. Ruth Waddell for her tremendous support and assistance in this project. She gave up much of her own time working out difficulties with instruments, offered many helpful suggestions to make the project develop, and guided me through the thesis writing process. I would also like to thank Dr. Christina DeJong of the School of Criminal Justice for serving on my committee and being available to answer questions along the way.

I cannot thank Dr. Jay Siegel enough for providing the idea for the project, continuing to play an active role in my pursuit of the degree, and accepting me into the Forensic Science program at Michigan State University. Most importantly, I extend my extreme gratitude to him for being both a friend and mentor to me.

There were several individuals who assisted me in various aspects of the project. I would like to thank Dr. Dan Jones and Bev Chamberlain of the Mass Spectrometry Facility who took the time to help me understand the MALDI-MS technique, and also how to operate the instrument. In addition, Dr. Ewa Danielewicz of the Center for Advanced Microscopy answered several questions I had regarding SEM-EDS, and I am extremely grateful for her assistance. I would also like to thank Monique Lapinski for allowing me to use her SEM beam time.

Throughout the course of this project many attempts at other techniques were made, and due to instrumental errors, were unable to be used. However, Dr. Kathy

Severin spent a tremendous amount of time with me working on the various instruments, and I would like to thank her for giving up her own time to help me.

I would like to thank friends and family for their continued support throughout my years at MSU. I would especially like to say thank you to my mother, Susie Patching, who not only purchased many of the powder samples for me, but was also there for me whenever I needed her.

Most importantly, I would like to thank my husband Dan Greenough for being my best friend and biggest fan.

TABLE OF CONTENTS

LIST OF TABLES

LIST OF FIGURES

1. INTRODUCTION

1.1 Cosmetics

Ancient Egyptians used cosmetics as early as 4000 BC, a trend that was continued throughout history by several different civilizations. Ancient Greeks and Romans applied makeup in order to attract attention and to signify class standing. In our society today, cosmetics continue to be used, applied to the eye area, fingernails, lips, or overall face, typically to increase attractiveness.

The term "cosmetic" is defined by the Food and Drug Administration (FDA) as:

> (1) articles intended to be rubbed, poured, sprinkled, or sprayed on, introduced into, or otherwise applied to the human body or any part thereof for cleansing, beautifying, promoting attractiveness, or altering the appearance, and
>
> (2) articles intended for use as a component of any such articles; except that such term shall not include soap. [1]

Cosmetics that are blended into the skin to even out skin tone have persisted throughout history. Currently, a variety of cosmetics can help achieve the look of flawless face, including foundations, concealers, and powders. Foundations are typically liquid based, formulated to match skin tone, and are rubbed into the entire facial region to reduce uneven skin tone. Concealers are also liquid based and skin colored, but are generally used only to cover blemishes, rather than the whole face. Powders are also matched to skin color, but their main purpose is not to cover redness or blemishes, but to decrease sheen that may occur due to oils in the skin. As with foundations, powders are also generally applied over the entire face, although are more easily reapplied throughout the day.

Today, there are thousands of foundations, concealers, and powders produced by different manufacturers and available in numerous shades to match the natural skin color. Due to their widespread use in our culture, these foundations and face powders can easily be transferred onto cloth or skin during the course of a crime and hence are an important type of trace evidence. The aim of this research is to characterize a number of commercially available face powders using a variety of analytical techniques, in order to assess the potential to differentiate powders according to manufacturer and brand.

1.2 Cosmetic Face Powders

Cosmetics may contain hundreds of different components, and federal regulations require ingredients to be listed on product labels in descending order by quantity.[1] However, the federal government relies heavily on industry self-regulation.[1] Unfortunately, the exact formulation is often proprietary and therefore ingredients within a cosmetic may not be listed on the product label. The label might contain only a partial list of ingredients, or a special listing of what "may" be contained in a product. Fatty acids, waxes, and oils are typically present in cosmetics. Oils present include lanolin, aloe, castor oils[2,3], while waxes commonly include beeswax, paraffins, and candelilla.[2,3] The color of cosmetics is provided by pigments and dyes such as D&C Red dyes, dihydroxyacetone, titanium dioxide, mica, and iron oxides[1].

While liquid based makeup products, such as the creams and lotions mentioned previously, contain an abundance of oils and waxes, cosmetic face powder has a different formulation which results in a different texture. The most common ingredient in face powders is talc ($Mg_{33}Si_4O_{10}(OH)_2$), which is not typically found in liquid products. In addition, powder lacks many of the oily components and preservatives found in

foundations. Other ingredients commonly found in powder samples include: titanium dioxide, zinc stearate, parabens, octyldodecyl stearoyl stearate, palmitate, aloe extracts, mica, calcium carbonate, silica, dimethicone, and mineral oil. Titanium dioxide, mica, and calcium carbonate are used as opacifying agents, for their covering power, brilliance, and reflectivity.[4] Parabens are a group of preservatives added to cosmetics for an antimicrobial effect, while dimethicone, or polydimethylsiloxane (PDMS) is a silicon-based organic polymer that gives a smooth feel to a cream, lotion, or powder.[1] Octyldodecyl stearoyl stearate is an ester that functions as a skin-conditioning agent, and a viscosity increasing agent.[5] The listed ingredients are found in nearly all powders, but each powder contains many more compounds, some that are listed on the product label, and others that are not. In addition, there is typically no listing of the proportion of each ingredient contained within that powder. Therefore, the exact composition of cosmetic face powders is not easily determinable from the product labeling; in fact, the exact composition is often known only by the manufacturer.

1.3 Forensic Analysis of Cosmetics

Several studies in the forensic science field have focused on the evidentiary value of cosmetics. To date, the primary focus has been on lipsticks, eye shadows, and nail polish, however, studies involving mascaras, sunscreens, and foundations have also been conducted. [2,6-11] These studies have used a variety of instrumental techniques to either differentiate or categorize cosmetics based on differences in their chemical composition. Choudhry and colleagues examined lipstick by microspectrophotometry (MSP) in the visible region and scanning electron microscopy-energy dispersive spectroscopy (SEM-EDS). Both techniques offered a rapid means of sample discrimination.[7] MSP was able to

differentiate lipstick samples of similar color but with minor shade differences that were invisible to the naked eye. SEM-EDS provided information regarding the elemental composition of the samples, and provided images of pigment particle morphology.[7] Both the elemental compositions and particle morphology of lipsticks provided discrimination ability. Ehara and Marumo performed a large study of 174 lipstick samples using purge-and-trap gas chromatography (P&T-GC) to analyze lipstick smears and identify them based on differences in oil composition.[12] Each sample was first observed under white light, and those samples that visually could not be separated based on color were classified in the same group.[12] The fluorescence of each sample was next observed using light at wavelengths of 350, 445, and 515 nm, P&T-GC.[12] The measurement of fluorescence at these wavelengths enabled discrimination of dyes within the lipstick samples. P&T-GC was used as a direct analytical technique for lipstick smears on filter paper, and the results were based on chromatographic peaks characteristic of the oils in each sample.[12] Using this technique, 174 samples could be classified into 48 groups.[12] The lipsticks that originated from the same manufacturer often produced chromatograms that could not be distinguished from one another.[12] Combining this technique with fluorescence and visual observation, the researchers were able to discriminate 15,038 lipstick pairs of samples out of 15,051, which corresponds to 99.9% of samples analyzed.[12]

Thin-layer chromatography (TLC) is a simple and economic technique that has proven to be useful when studying cosmetics, particularly lipstick, due to its ability to separate dye components.[13-15] Singh and Jasuja analyzed 15 liquid lipstick samples of different brands applied to a variety of substrates such as glass, filter paper, tissue paper,

and skin.[14] The dry samples were lifted from the surfaces with cotton swabs moistened with alcohol, and the stains were then dissolved in toluene before being spotted on a TLC plate.[14] The authors were able to develop a solvent system that allowed separation of dye components and differentiation of the lipstick samples.[14] TLC is a valuable screening technique, simple and rapid, yet it has limitations in its selectivity, and thus cannot be used as a confirmatory test.

Several thesis projects performed at Michigan State University have characterized different cosmetic types for forensic purposes.[2,6,10] Mascaras were analyzed using microscopy, Fourier transform infrared spectroscopy (FTIR), SEM-EDS, and MSP to determine an appropriate protocol for analysis of such samples.[6] Microscopy grouped the 24 mascara samples into 4 groups based on particle colors, and presence or absence of fibers that are sometimes added to mascara to increase the length of eyelashes when applied.[6] However, visual observation and determination of color is subjective, and fiber presence may be due to transfer. It was therefore concluded that microscopy was useful as a preliminary screening tool.[6] Microscopy was then followed by FTIR spectroscopy, which can identify functional groups in samples and allow for the comparison of samples based on chemical composition.[6] FTIR was able to distinguish 21 of the 24 samples from each other based on the presence of major peaks in the IR spectra.[6] The third technique, SEM-EDS, allowed differentiation of samples based on elemental concentrations.[6] Based on the comparison of elemental weight percentage of the samples, SEM-EDS could distinguish 99.67% of samples.[6] The last technique, MSP, did not provide any discriminatory data for the analyzed samples, due to the black color of mascara.[6]

In addition to the mascara research, a project to determine an appropriate protocol for analysis of nail polish was also performed.[10] Romero studied 20 nail polishes varying in color and manufacturer using microscopy, MSP, and FTIR spectroscopy.[10] Microscopy was able to distinguish between each of the nail polishes, with the exception of five. These five were from the same manufacturer, but different lots.[10] Three of the five samples could not be distinguished by MSP, but were distinguished by microscopy.[10] When compared to a IR spectral library of lipstick samples, the correct lipstick was identified 96% of the time.[10] This study determined that, in order to determine a match between a questioned and known sample, microscopy should be the first step in analysis, followed by MSP, then reflectance FTIR for samples where quantity is limited.[10] This combination of techniques allows more confidence in discriminating samples compared to a single technique which, as shown in this study, has limited discriminating power.[10]

A thesis project performed by Stark combined the techniques of MSP, laser desorption ionization mass-spectrometry (LDI-MS), and FTIR spectroscopy to classify 57 lipsticks.[6] MSP grouped the lipsticks into 5 spectral classes based on their wavelength of maximum absorbance. IR spectra of the lipstick samples were compiled to create a library of spectra, and then the spectra were re-collected, and compared to the library. For this method, the top ten possible matches were listed.[2] Forty-eight lipsticks yielded accurate search results, where the correct lipstick was the number one match, while the other samples matches were all in the top ten.[2] Mass spectra of the lipstick samples were obtained by LDI-MS and classification was performed based on presence or absence, as well as the identity, of predominant peaks.[2] The initial assessment grouped the samples into five general groups, then further classification into smaller sets was performed

within each of the groups. Within each group, distinctions between most of the lipsticks could be made based on additional peaks present within the spectra.[2] Some of the peaks found in the mass spectra could be identified as components of castor oil, a common ingredient in lipsticks, and known dyes such as D&C Red 27 .[2] Other peaks within the spectra could not be identified as known ingredients.

While the characterization of various cosmetics has been published in the literature, few studies deal with cosmetics that have the specific function to even out skin tone, such as foundations, concealers, and powders. Gas chromatography-mass spectrometry (GC-MS) was used in an early study of castor oil-based cosmetic powders, creams, and lotions[9], and a recent study examined the ability to discriminate between different types of foundations using a combination of methods.[8] A study performed by Gordon and Coulson in 2004 focused specifically on liquid foundations. Foundations were smeared on three different types of fabric, and the smears were analyzed by FTIR, GC with flame ionization detection (FID), and SEM-EDS[5]. A total of 53 samples were considered. Twenty-three pairs out of the 1378 possible pairs could not be distinguished with FTIR, yielding a discrimination power of 98.3%.[8] GC-FID alone yielded a discrimination power of 82%, or 1130 pairs distinguished out of 1378, and SEM-EDS discriminated all but 83 pairs out of the possible 1378, for a discrimination power of 94%.[8] The three techniques when combined, resulted in a discrimination power of 99.7%.[8]

1.4 Research Objectives

The proposed research aims to firstly characterize cosmetic face powders using SEM-EDS, FTIR, and matrix-assisted laser desorption ionization mass spectrometry (MALDI-MS) and then assess the discrimination ability of each technique in differentiating the face powders. Currently, no studies are available that analyze and characterize face powders and thus it is believed that this work will contribute to the significance of cosmetics as forensic evidence.

A total of 27 face powders were examined by SEM/EDS, FTIR, and MALDI MS. Each of these methods provide complementary information about cosmetic samples. SEM-EDS can produce images so the morphology of samples can be compared, and can provide an elemental profile of the samples, yielding the atomic percentage of each of the various elements within the samples. These atomic percentages can be statistically compared among samples for comparison. FTIR spectroscopy can provide information about the chemical functional groups present in the samples which can be used to identify components present in the samples. The presence or absence of major peaks in the spectra can be used to visually assess the similarities and differences between samples. MALDI-MS can provide information about qualitative and quantitative composition of both organic and inorganic components in the face powders, and can yield structural information of the species within and each sample.[16] The ability of the techniques to discriminate the face powders will be investigated, individually and in various combinations. By characterizing the chemical composition of the face powders using a variety of techniques, successful discrimination of samples may be possible increasing the significance of such evidence in forensic casework.

CHAPTER 2 INSTRUMENTAL THEORY

2.1 Scanning Electron Microscopy/Energy Dispersive Spectroscopy (SEM-EDS)

2.1.1 Introduction

Scanning electron microscopy-energy dispersive spectroscopy has proven to be a useful tool in the field of forensic science, as it can provide both qualitative and quantitative information of the inorganic components of samples.[17] The scanning electron microscope (SEM) in particular is often found in forensic laboratories and provides powerful magnification (10X to 100,000X), a large depth of field, and high resolution when compared to a light microscope.[17] In addition, when combined with energy dispersive spectroscopy (EDS), SEM has the capability to identify and quantify elements within a sample.

2.1.2 Scanning Electron Microscopy

The magnification and imaging ability of the SEM allows the morphology of samples to be visually examined, allowing sample differentiation based on morphology.

Samples must be prepared for the SEM so that they contain no volatiles, are firmly mounted, and are electrically conductive. Samples are mounted in aluminum stubs, attached by either carbon cement, epoxy glue, or adhesive tabs, then sputter coated, typically with gold or carbon to make the samples conductive. Once conductive, the samples are placed into the instrument chamber.

An SEM is composed of the following basic parts[17]: the electron gun, condenser lens, scan coils, objective lens, final aperture, scintillator, detector, computer, and cathode ray tube (Figure 2.1.1)

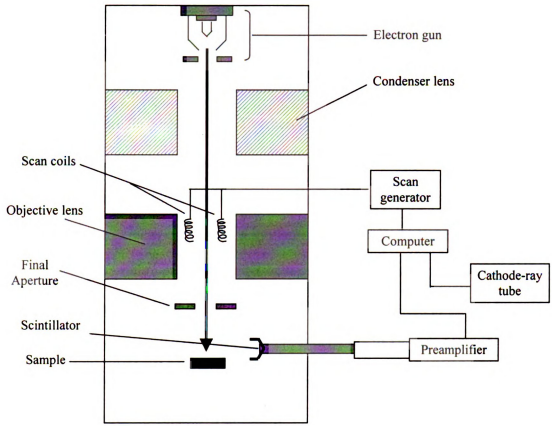

Figure 2.1.1. Diagram of SEM

The electron gun produces a beam of electrons that is condensed by the condenser lens. The scan coils within the objective lens create a magnetic field that deflects the electrons towards the sample. The electrons are focused and the electron beam then strikes the sample.

When the electron beam interacts with the sample, a series of interactions occur, producing secondary electrons (SE). When the beam interacts with the orbital shells of atoms in the sample, the electron within the beam are scattered. When this occurs, the path of the beam is deflected by a small angle, resulting in energy loss. This type of interaction is called inelastic scatter and results in a low energy (3-5 eV) electron being ejected from the atomic orbital. Any electron detected as a result of sample-beam

interactions that has energy of less than 50 eV is a secondary electron. Most secondary electrons do not have enough energy to escape from the sample, unless they are located near the surface of the sample, within approximately 50 nm.

Common detectors for SEM include Everhart-Thornley (ET) detectors which are composed of a Faraday cage, scintillator, and photomultiplier tube (PMT). Secondary electrons emitted from the sample are attracted to the Faraday cage, which is maintained at ~ +300 V. Behind the Faraday cage is the scintillator, which typically has a thin coating of conductor material to maintain the positive voltage.[18] Electrons are accelerated to a +12000 V charge on the scintillator and, upon striking the scintillator, photons of light are produced that are then directed into the PMT. Inside the PMT, the photons' interactions with electrodes causes an amplified emission of electrons that are sent to the cathode ray tube to produce 3D images of the sample.

The images obtained by SEM result from the differences in amounts of secondary electrons from flat portions of the sample versus projections on the sample. The flat regions are seen as dark images on the cathode-ray tube, while projections yield brighter spots. This is a direct result of secondary electrons' ability to escape the sample surface. When topographical features are present on the sample, a greater volume is close to the surface. In such an area, the secondary electrons are close to the surface, and can escape, thus creating a brighter image.

Although secondary electrons account for the majority of interactions that produce the SEM image, other types of interactions occur between the sample and the electron beam. Elastic scatter, which can occur between incident electrons and the nucleus of atoms in the sample,[17] is characterized by a large-angle deflection of the

incident electron beam, as well as little energy loss by the incident electrons.[17] Some elastic scatter produces backscattered electrons (BSE), which are those electrons eventually scattered at ~180° to the incident electrons. Unlike secondary electrons, backscattered electrons have energies on the order of kV, similar to the energy of the incident beam, allowing escape from much greater depths within the sample. They can provide an atomic number image as well as a depth image.

2.1.3 X-ray Production

Along with secondary and backscattered electrons, interaction of the electron beam with the sample can also result in the emission of X-rays, as electrons from higher energy shells fall to fill the vacancy created by the initial interaction (Figure 2.1.2). Due to the quantized nature of atomic energy shells, the energy of the x-ray emitted is characteristic of the atom and related by Equation 2.1, where λ is the wavelength in nanometers, and E is the energy in keV.[17]

$$\lambda = \frac{1.2398}{E} \qquad \text{(eqn. 2.1)}$$

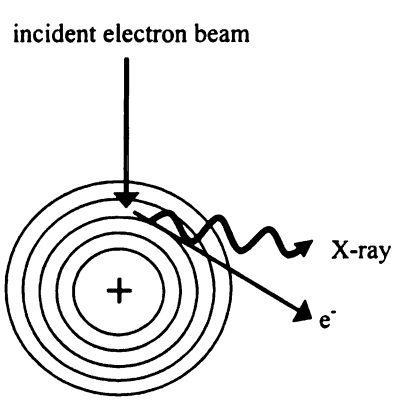

Figure 2.1.2 Inelastic scatter resulting in an x-ray.

With the SEM coupled to an energy dispersive spectrometer (EDS), the x-rays emitted following interaction of the electron beam with the sample are detected. Since the energy of the emitted x-ray is characteristic of the atom, elemental composition of the sample can be determined.

The critical excitation energy, also known as the absorption edge, is the beam energy needed to eject an electron from an atomic shell. With an electron ejected, a vacancy now exists in the shell, and the atom is unstable. To restore stability, an electron from a higher shell falls to fill the vacancy, emitting an x-ray as it does so. Each type of X-ray is called a line, and if sufficient x-rays of a given line are generated, they produce an x-ray peak in the spectrum. If the critical excitation energy is not sufficient to remove an electron from a given shell, then no x-ray lines are seen.[17] The difference in critical excitation energies for different elements gives rise to differences in the analytical spatial resolution when analyzing for specific elements.[17]

X-rays are named according to the atomic shell where the vacancy exists, and the number of jumps made by the electron to fill that vacancy. The atomic shells are named K, L, M, and N, where K is the inner shell, closest to the nucleus, followed by L, M, and N.

If the electron falls one shell to fill the vacancy, the emitted x-ray is called an α x-ray, falling two shells results in a β x-ray being emitted, and falling three shells to fill the vacancy would be termed a γ x-ray. For example, if there was a vacancy in the L shell of an atom and an electron from the N shell falls to fill the void, then the electron has fallen two shells. Since the vacancy existed in the L shell and involved an electron falling two shells to fill the vacancy, the emitted x-ray is an L_β x-ray (Figure 2.1.3).

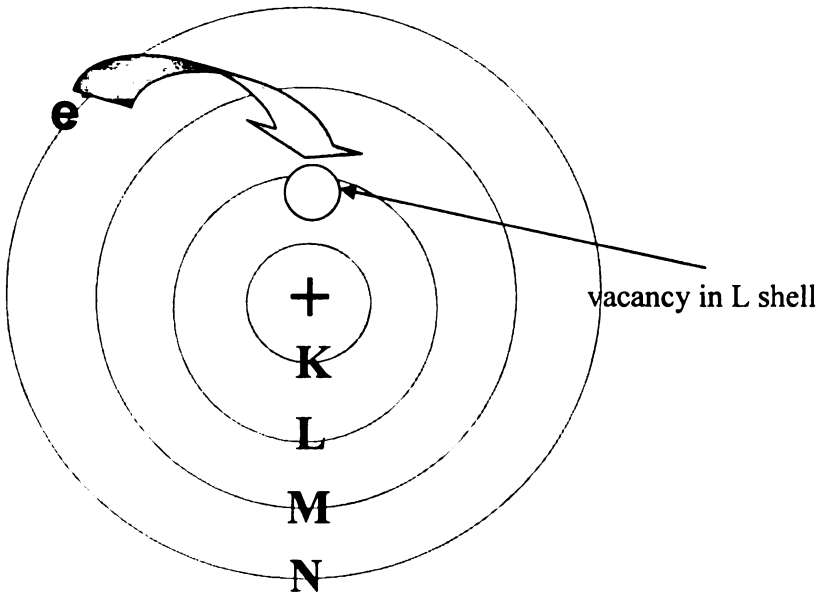

Figure 2.1.3 An electron from the N shell fills a vacancy in the L shell, resulting in the emission of an L_β x-ray.

2.1.4 X-ray Detection

The energy of the emitted x-rays can be detected via energy dispersive spectroscopy (EDS). Since the x-ray energies are characteristic of the elements present, EDS allows elemental identification.

The EDS detector is designed to convert the energy of each individual x-ray emitted into a voltage signal of a proportional size.[19] The EDS detector (Figure 2.1.4) consists of the following main components: collimator, crystal, field-effect transistor (FET), pulse processor, analog-to-digital converter, multichannel analyzer.

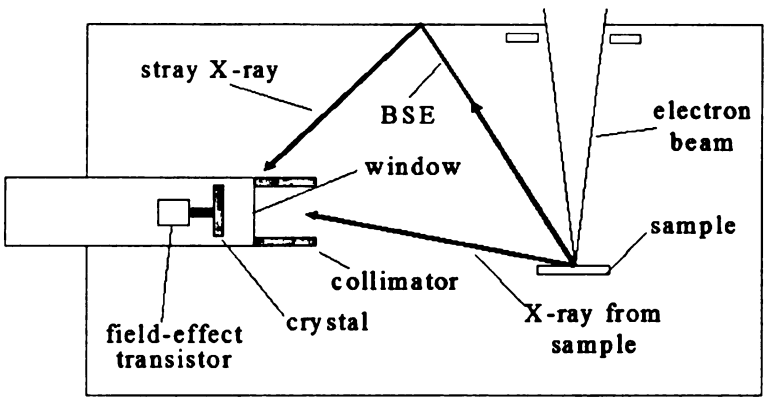

Figure 2.1.4 The EDS detector

The carbon-lined collimator contains internally mounted magnets that absorb stray radiation. Following the collimator is a thin membrane window that serves as a barrier and prevents contamination of the detector crystal, which is composed of silicon and lithium.[17] The crystal, which has a 1000 V bias, converts each x-ray into a charge by the ionization of atoms in the semiconductor crystal.[19] The charge is then converted into a voltage signal by the FET pre-amplifier.[19] The voltage signal is sent to a pulse processor for measurement.[17] The number of pulses produced corresponds to the energy of the incoming x-ray. The analog-to-digital converter takes each pulse from the pulse processor and converts it into a series of pulses of equal height.[17] The number of pulses corresponds to the height of the original pulse and to the energy of the x-ray.[17] The multichannel analyzer places the pulses into channels of varying energy which, through the computer and cathode ray tube, displays the energy spectrum. The resulting spectrum is plotted as intensity or counts on the y-axis and x-ray energy (in keV) on the x-axis (Figure 2.1.5).

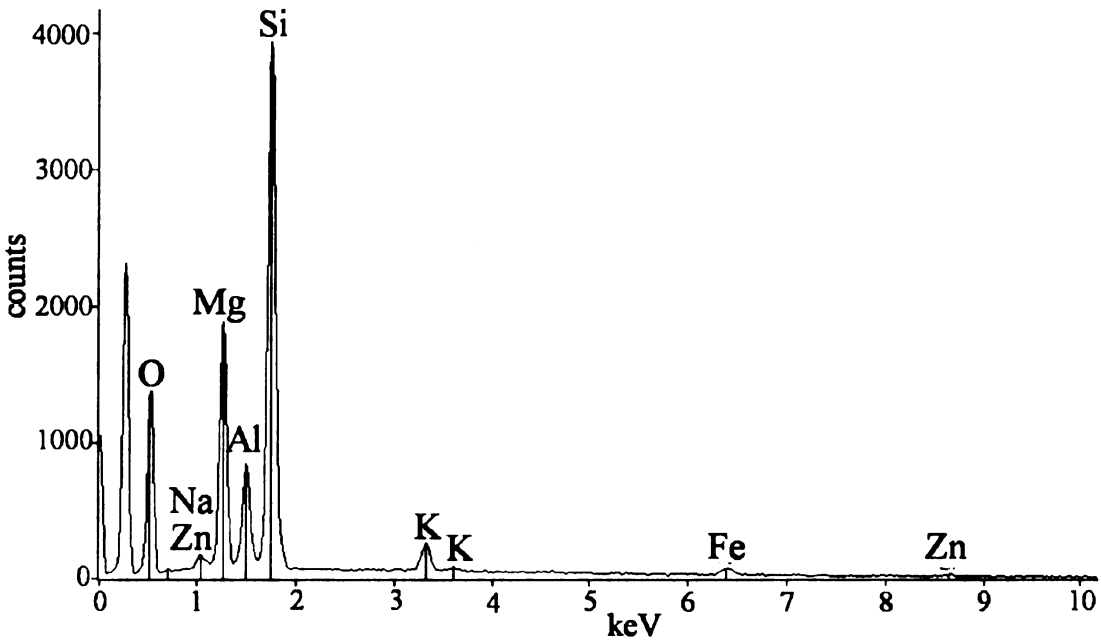

Figure 2.1.5 Example of an EDS x-ray spectrum

2.1.5 SEM/EDS

SEM combined with EDS is an effective analytical technique. The secondary electrons produced from the sample make it possible to collect high resolution images, giving detailed sample morphology, while the EDS detector allows qualitative and quantitative analysis of elemental composition within the sample.

The combination of SEM images and EDS make this technique particularly effective when analyzing cosmetic samples since complementary information can be obtained in a single analysis. In this work, the morphology of the face powder samples was compared by SEM. Elemental composition was determined by EDS and the element weight percentages were calculated for comparison of samples.

2.2 FOURIER TRANSFORM INFRARED SPECTROSCOPY

2.2.1 Introduction

Infrared (IR) spectroscopy is a technique in which infrared radiation is directed through a sample and, depending on the chemical structure of the sample, various wavelengths of IR light are absorbed, allowing sample identification. The infrared region of the electromagnetic spectrum is between 12800 cm^{-1} and 10 cm^{-1}, and is further divided into the near IR (12800 cm^{-1} – 4000 cm^{-1}), mid IR (4000 cm^{-1} – 200 cm^{-1}), and far IR (200 cm^{-1}– 10 cm^{-1}) regions. The mid IR region is the most useful for identifying functional groups in the sample and to provide both qualitative and quantitative information. Within the mid-IR region, functional groups display absorbances in the 4000-1500 cm^{-1} region, while the region from 1200 cm^{-1} to 600 cm^{-1}, called the "fingerprint region" displays peaks characteristic of certain molecules, potentially allowing definitive identification of the sample.

2.2.2 Molecular Interactions with IR Radiation

Infrared light is low energy and therefore excites vibrational modes of a molecule. There are two types of vibrations within a molecule: bending modes and stretching modes. For a substance to absorb IR radiation, the molecule in question must undergo a net change in dipole moment as a consequence of the incited vibrational motion. Therefore, the bonds within the molecule must have a permanent dipole moment to absorb IR light. Molecules including homonuclear diatomics and some simple inorganic salts do not absorb in the mid IR region, but many organic functional groups do have the required dipole moment and will absorb infrared light.

Every molecule has natural vibrational frequencies based on the functional groups present in the molecule. Because vibrational energy levels are quantized, there are particular frequencies associated with transitions between energy levels for different types of bonds and functional groups (Appendix A). When the molecule absorbs infrared light with a frequency that corresponds to the energy between two levels, the molecule is vibrationally excited, an increase in the amplitude of absorbance occurs, and peaks are seen in those regions on the infrared spectrum. Typically, the presence or absence of major peaks in the region from ~4000 cm^{-1} to ~1500 cm^{-1} can yield information about the functional groups present in a particular samples, and differentiation of samples can be made based on such visual comparison of the corresponding IR spectra.

The "fingerprint" region of an IR spectrum is between ~1200 cm^{-1} and ~600 cm^{-1}. This region of an IR spectrum is often more complicated than in the region above 1200 cm^{-1} because these absorptions are mainly due to bending modes rather than stretching modes within the molecule. Different molecules have unique vibrations in this region, allowing definitive identification of the molecule.[20] However, when classifying groups of compounds based on IR, it is often easier to first examine the "cleaner" region from 4000 cm^{-1} to ~1200 cm^{-1} and determine whether samples can be grouped based on the presence or absence of major peaks.

2.2.3 Fourier Transform Infrared Spectroscopy

Fourier transform infrared (FTIR) spectrometers now constitute the majority of the instrument market compared to the older type dispersive instruments. The FTIR spectrometer offers the advantages of improved signal-to-noise, speed, resolution,

accuracy, and reproducibility. The main advantages of FTIR is that it has the ability to scan all wavelengths simultaneously, resulting in rapid analysis, and it converts data from the time domain to the frequency domain.[16] Rapid scanning of all wavelengths is accomplished by the use of a Michelson interferometer, as shown in Figure 2.2.1.

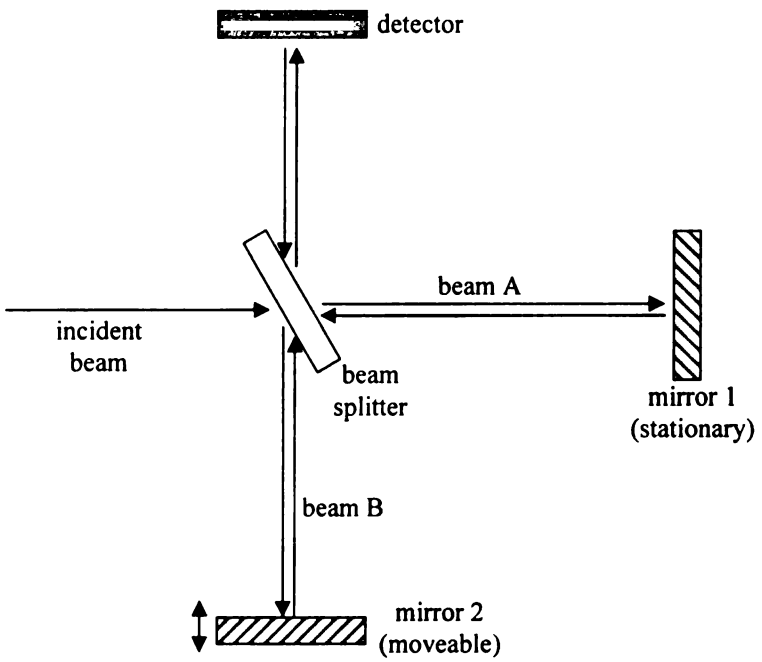

Figure 2.2.1 A Michelson interferometer

The incident IR beam encounters a beam splitter where the beam is divided, with half of the beam traveling to a stationary mirror and the other to a moveable mirror. The beam is reflected from both mirrors back to the beam splitter, where it recombines and passes to the detector. However, due to the moving mirror, the two half beams have traveled different pathlengths, resulting in interference patterns as the two recombine. When the distance from the beam splitter to the moveable mirror is equal to the distance between the beam splitter and the stationary mirror the pathlengths are the same, resulting in constructive interference when recombined.[16,20,21] When the moveable mirror is moved a

distance of $\lambda/4$ from the beam splitter, the beam traveling towards this mirror must travel a distance of $\lambda/2$ greater than the beam traveling to the stationary mirror.[16,21] The result is destructive interference when the beams are recombined, and no signal is detected. Due to the constructive and destructive interference on recombining the beam, an interferogram is produced when the moveable mirror is scanned at a constant velocity. The recombined beam passes through the sample, which absorbs at all the frequencies characteristic of the functional groups present. The frequencies absorbed are subtracted from the interferogram and the beam passes to the detector, which records variation in energy versus time for all wavelengths simultaneously.

A mathematical function, the Fourier transform, is used to convert the interferogram, which is measured in the time domain, into the absorbance spectrum, which is in the frequency domain. The period of the interferogram is related to the center frequency that is seen in the spectrum and the interferogram's exponential decay is related to the linewidth of the peaks in the spectrum.

2.2.4 Attenuated Total Reflection

Attenuated total reflectance (ATR-FTIR) uses a sampling accessory that has been shown to be reproducible for qualitative and quantitative analysis of liquid, paste, solid, film, and powder samples that range from organic to inorganic in nature.[22] While a transmission IR measurement collects a spectrum that is an average of the bulk properties of the sample, ATR measurements only measure surface properties of the sample because the IR beam only penetrates a short distance into the sample.

An ATR accessory typically consists of a sampling plate in close contact with a high refractive index crystal such as diamond, zinc selenide, or germanium. The solid

sample is placed on top of the sample plate and pressure is applied to the sample to ensure good contact between the sample and the crystal (Figure 2.2.2) .[16]

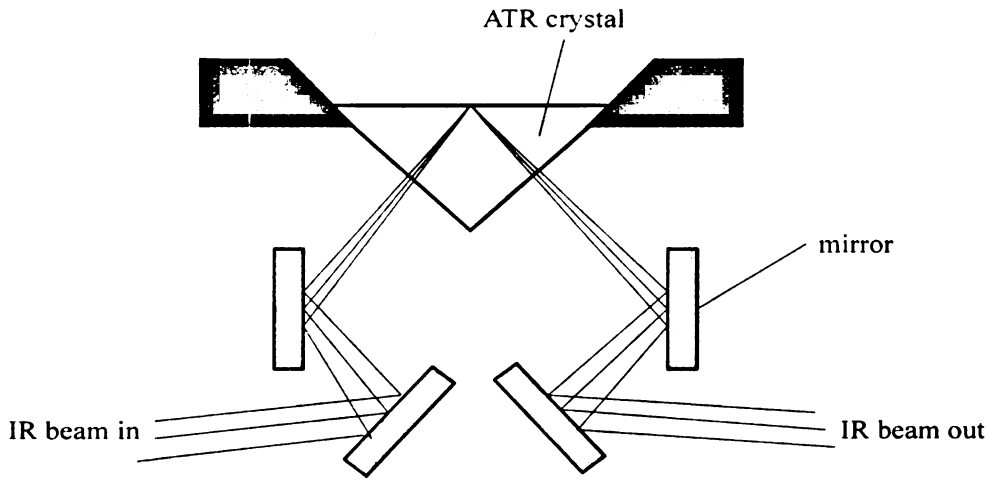

Figure 2.2.2 Diagram of a single-bounce ATR accessory

IR radiation is directed into the crystal at an angle exceeding the critical angle for total internal reflection.[22] The high refractive index of the crystal allows the radiation to reflect within the ATR element rather than be transmitted. The fraction of the beam that is reflected increases with the angle of incidence, θ_i. When the incident angle is greater than the critical angle, the beam is completely reflected. When an absorbing sample is brought into contact with the crystal, the incident beam penetrates a small distance into the sample before reflection occurs.[16,21] The distance the beam protrudes beyond the surface of the crystal and into the sample is the penetration depth which is dependent on the wavelength of the incident light. With IR radiation, the penetration depth is typically only a few microns deep. However, the penetration depth is also dependent on the refractive

index of the medium, the angle of incidence, and the wavelength of the incident beam of light. On penetrating into the sample, frequencies of IR radiation corresponding to energies of vibrations of chemical bonds in the sample are absorbed. A spectrum of absorption versus frequency is produced in the same manner as FTIR, allowing sample identification. The absorbances, although dependent upon the angle of incidence, are independent of sample thickness because the radiation penetrates only a few micrometers into the sample.[16]

A major concern when using ATR is that, while the same peaks are observed on an ATR spectrum as with transmission FTIR, their intensities are often weaker. Therefore, some of the detail may be obscured in ATR-IR spectra. This is most likely due to the penetration depth. Since penetration depth is dependent on the wavelength of the incident light, absorbance bands at shorter wavelengths (infrared region) will be of lower intensity that those of longer wavelength.

A major benefit of using ATR is that there is no sample preparation; the sample can simply be placed upon the ATR crystal which is cleaned thoroughly between samples. In this research, the sample introduction method is particularly useful because it is difficult to make a transparent KBr disk with opaque samples and samples like face powders that contain anti-caking agents. In addition, ATR is a technique commonly used in forensic labs. In this work, ATR-FTIR was used to qualitatively determine the organic components present in the face powder samples.

2.3 MATRIX-ASSISTED LASER DESORPTION IONIZATION-MASS SPECTROMETERY

2.3.1 Introduction

The field of mass spectrometry blossomed in the second half of the twentieth century.[16,23] The basic principle behind the technique was that a sample solution was evaporated into the gas phase, the molecules were then ionized, and the resulting ions separated and analyzed based on their mass/charge (m/z) ratio. Since the introduction of mass spectrometry as an analytical technique, a number of different sample ionization methods have been developed, for example electron impact ionization (EI), chemical ionization (CI), or electrospray ionization (ESI). However, larger molecules (>1000 Da) were difficult to analyze utilizing CI and EI, mainly due to difficulties in evaporating the sample solution; on heating, the sample would decompose rather than evaporate. To overcome this obstacle, instantaneous evaporation must occur. A solution to this problem was discovered in the 1980s, with the introduction of matrix-assisted laser desorption ionization (MALDI).

2.3.2 MALDI

MALDI is a laser ionization method in which a short, intense laser pulse is used to ionize the analyte molecules. This is achieved in two steps. First, the compound that is to be analyzed is mixed with an organic matrix on a solid sampling plate.[23] Several matrices are available for MALDI analyses, with the choice of matrix dependent on the laser wavelength used. The molar ratio of analyte to matrix in the mixture is typically ~1:10,000. The sample-matrix mixture is allowed to dry on the plate, resulting in a spot of analyte-doped matrix.[23] The plate is then placed in the sample chamber, which is

evacuated to the operating pressure of the instrument. The laser is then fired at the sample-matrix spot in short pulses, resulting in the ablation of bulk portions of the sample-matrix spot. The laser pulses are in the order of ~10 μJ and are focused on a small diameter spot (~100 μm) resulting in intense heat on the surface of the sample spot. This rapid heating causes rapid sublimation of the matrix crystals, leaving the analyte molecules intact in the expanding matrix (Figure 2.3.1).[23]

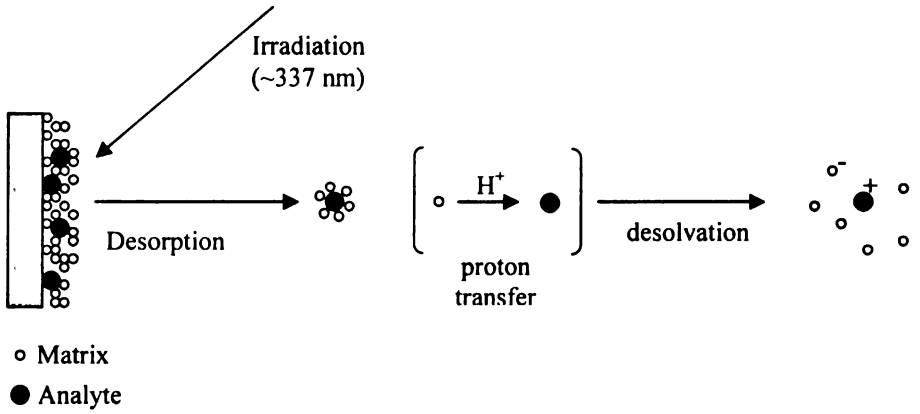

Figure 2.3.1 The principle of MALDI

Although the exact mechanism of ionization is not well understood, the process produces gaseous molecules of matrix and analyte, ion pairs, and ions of both matrix and analyte. Both positive and negative ions of the initial analyte are produced and hence, either the positive ion mode or negative ion mode of detection can be selected.

The ions produced are then focused using a series of electrostatic lenses into the mass analyzer. A time-of-flight (TOF) mass analyzer is typically used for pulsed ion sources, and is therefore often utilized with MALDI-MS.[23] The linear TOF analyzer has been used since the 1950s, and consists of a flight tube, approximately 1 meter in length (Figure 2.3.2).[23]

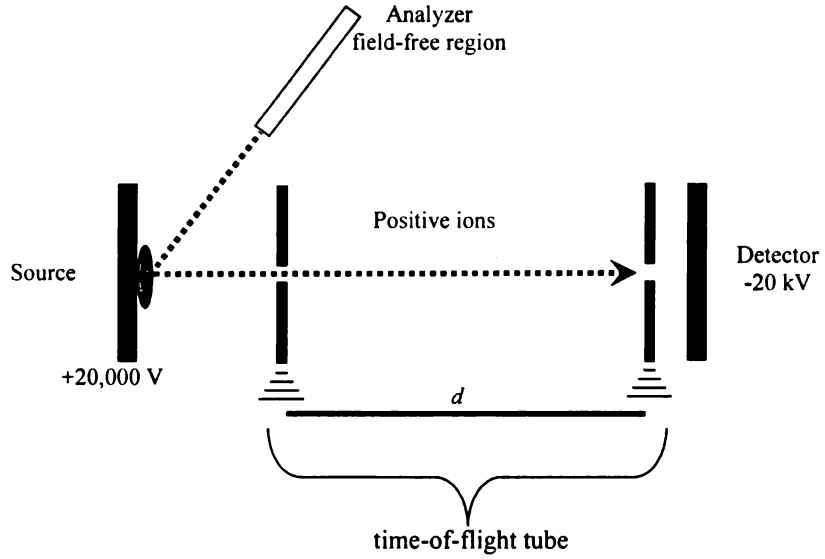

Figure 2.3.2 The time-of-flight mass analyzer

The ions are accelerated from the sample chamber into the TOF tube by an applied electric field and are imparted with kinetic energy (KE):

$$KE = \frac{mv^2}{2} = zeV_{acc} \qquad \text{(equation 2.3.1)}$$

where m = mass (kg), v = velocity (m/s), z = charge, V_{acc} = accelerating voltage (V), and e = elementary charge (1.6×10^{-19} C). The ions then enter the flight tube and are separated according to the time taken to drift down the tube in a field-free region. The drift time of the ions is dependent on their size, or mass-to-charge ratio (m/z) as shown in equation 2.3.2:

$$v = \sqrt{\frac{2zeV_{acc}}{m}} \qquad \text{(equation 2.3.2)}$$

Larger, heavier ions take longer to migrate the length of the tube than smaller, lighter ions. Therefore, ions become separated according to their flight time.

At the end of the tube the ions strike the photographic plate detector, and the mass spectrum is obtained by measuring the signal as a function of time.[23] The time it takes for the ions to reach the detector, *t*, is the distance traveled, *d*, divided by the velocity, (*t=d/v)*. By substitution and rearrangement, the m/z can be determined by knowing the accelerating voltage, flight tube distance, and flight time, as shown in equation 2.3.3:

$$m/z = \frac{2t^2 eV_{acc}}{d^2} \qquad \text{(equation 2.3.3)}$$

2.3.3. Interpretation of Mass Spectra

The mass spectrum is a graph of ion intensity as a function of m/z (Figure 2.3.3).[24] This record of ions and their intensities serves to establish the molecular weight and structure of the compound being analyzed.[24]

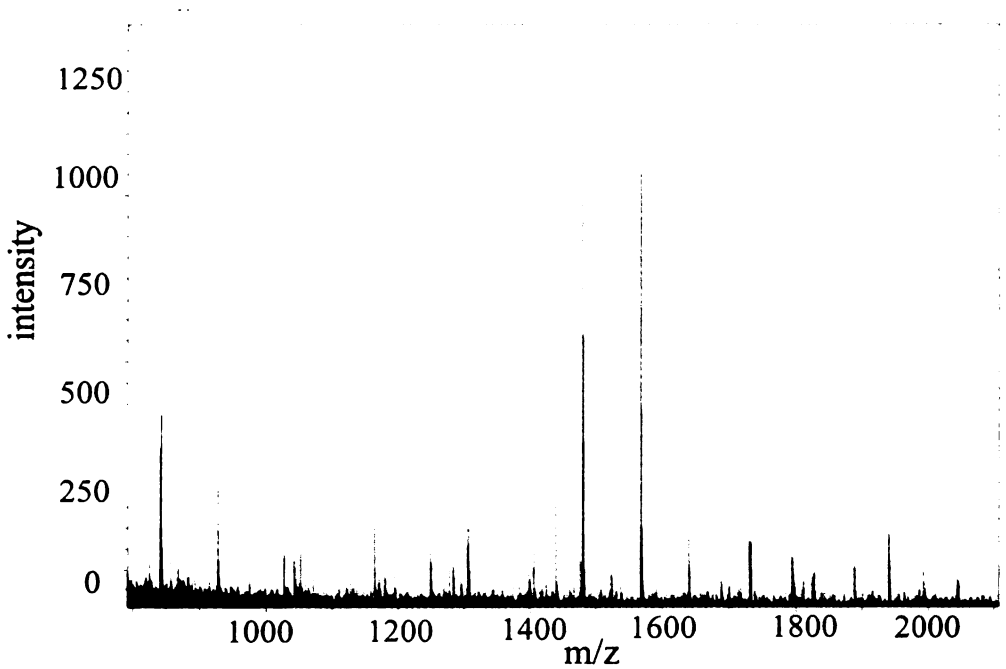

Figure 2.3.3 Example of a mass spectrum.[25]

Within a mass spectrum are several notable peaks. The base peak is the most intense peak in the spectrum and is assigned a relative intensity of 100%. The molecular ion results from ionization of the analyte molecule and appears at an m/z value numerically equal to the nominal molecular weight, or at one mass unit higher or lower than the molecular weight. The ionization process breaks up the analyte molecule into smaller fragments at certain bonds within the molecule. Once the analyte molecule breaks into fragments, each fragment has a different, lower m/z value. The fragments themselves will break up further in a similar manner. The pattern of fragmentation can often be determined by the peaks seen in the mass spectrum. In these cases, it may be possible to determine the structure of the analyte molecule from the mass spectrum based on the molecular ion and fragment ions.

MALDI-MS is typically utilized for analysis of complex biological samples that often include proteins or peptides and a great number of contaminants.[23] MALDI allows determination of the molecular weight of molecules up to 500 kDa.[23] The contaminants may include buffers, salts, detergents, and many other compounds of unknown origin.[23] Due to the complexity of samples often analyzed by MALDI-MS, the resulting spectrum is typically complicated with hundreds of different peaks, making structural identification difficult. Therefore, such samples are often first separated by chromatography, or tandem MS is performed. However, in this work neither of these options were available and face powder samples were compared based on a visual comparison of corresponding mass spectra.

CHAPTER 3 METHODS AND MATERIALS

A total of 27 face powders were examined in this research, totaling 351 different pairs of samples, where:

$$pairs = \frac{n(n-1)}{2} \qquad \text{(eqn. 3.1)}$$

Samples were either purchased or donated for the project, and varied in manufacturer, type of powder, and shade (Table 3.1.1). Due to the high cost of these products, a limited number of sample powders could be obtained. While 27 face powders represent only a small fraction of the products available, the samples obtained for this work provided seventeen different brands of powders to be compared. A complete ingredient listing for each powder sample is shown in Appendix B.

Table 3.1.1 Face powder samples

Sample	Brand	Type of powder (as described on label)	Color	Condition
1	Almay Luxury Finish	loose	ivory	new
2a	Revlon Skinlights		golden light	new
2b	Revlon Skinlights		golden light	new
2c	Revlon Skinlights		golden light	new
2d	Revlon Skinlights		golden light	new
3	Neutrogena Skinclearing Oil-Free	pressed	medium	
4	Almay Clear Complexion Light & Perfect	pressed	translucent	
5	Loreal True Match Super Blendable		Neutral	
6	Covergirl Clean		ivory	Used
7	Max Factor Colour Adapt	pressed	Light, pale	
8	Jafra Translucent		Blushing beige	Used
9	Prestige Perfectly Matte translucent		Honey	
10	Covergirl Clarifying		Natural ivory	
11	NYX Twin Cake		Honey beige	New
12	Le Mirador Instant			Used

Table 3.1.1, continued

	Infusion			
13	Covergirl Smoothers	pressed	Translucent	
14	Bonnie Bell Glimmer Bronze Luminous	loose	Gold 'n glitz	new
15	Jordana	pressed	natural	New
16	Maybelline Finish Matte	pressed	Medium beige	
17	Jane Bronzing		Sahara	
18	Wet 'n Wild	pressed	Ivory	
19	Estee Lauder Moisture Balanced Translucent		Beige	
20	Motives Color Swirl		Sun storm	Used
21	Covergirl (unknown)			used
22	Covergirl TruBlend	pressed	Translucent fair	used
23	Wet 'n Wild Ultimate touch	pressed	bare	Used
24	Wet 'n Wild Ultimate touch	pressed	natural	new

Some of the powders were labeled as either "pressed" powder or "loose" powder, while others had no designation. Samples 2a, 2b, 2c, and 2d were separate powders within the same compact. All of the powder samples were very fine, uniform powders, which could not be easily differentiated by the naked eye. Each sample was analyzed by SEM-EDS for morphology and elemental composition, and FTIR and MALDI-MS for information regarding organic components. The data from these techniques will be compared in order to determine whether these methods can be beneficial in distinguishing between the various sample powders. In addition, three samples (samples 2b, 21, and 22) were analyzed by each technique in triplicate to assess reproducibility of the techniques. Samples from three of the powders (samples 12, 17, 18) were re-analyzed and treated as "blind" samples to assess the discrimination and classification ability of each technique.

3.1 SEM-EDS

Adhesive tabs were attached to aluminum stubs, and approximately 1 mg of each powdered sample was placed on an individual stubs. The stubs were then coated with carbon using an Ernest F. Fullam Inc. EFFA MKII Carbon Coater. Although SEM samples are most often coated with gold, carbon was used instead because it has a very low absorption factor for x-rays.[17] Once the samples were prepared, the stubs were placed in a sample holder that held up to 4 samples at one time. The sample holder was then inserted into the SEM for analysis.

The scanning electron microscope used in this work was located in the Center for Advanced Microscopy on the Michigan State University campus. A JEOL (Japan Electron Optics Laboratories) 6400 V scanning electron microscope with a LaB_6 emitter (Noran EDS) coupled with a Thermo Electron Corporation X-ray Detector (Waltham, MA) was used for the analysis of all samples, using an accelerating voltage of 20.0 kV and a working distance of 15 mm.

For three samples, x-rays were collected at three different spots to ensure homogeneity, and x-rays from one spot was collected on the other samples. In addition, three samples (samples 12, 17, and 18) were selected as blind samples to test discrimination ability of this technique. The computer software program Noran System Six X-ray microanalysis system (Thermo Fisher Scientific, Inc., Waltham, MA) was used to identify the elements within the sample, and to provide quantitative results.

3.2 FTIR Spectroscopy

A Perkin Elmer Spectrum One FTIR spectrometer equipped with a mercury cadmium telluride (MCT) detector (Perkin Elmer, Shelton, CT) was used in this study.

The spectrometer was fitted with an attenuated total reflectance (ATR) sampling accessory containing a ZnSe crystal (Perkin Elmer, Shelton, CT). The spectrometer was operated and spectra were analyzed using the software program *Spectrum* (version 5.0.1, Perkin Elmer, Shelton CT).

The crystal and sample plate were cleaned with methanol prior to placing ~50 mg of powder sample directly on the sample plate. The exact mass of the powder used was not measured, but enough was used to completely cover the crystal with a measureable depth. Pressure was applied using the pressure arm, and the software program provided a pressure bar that measured the actual pressure imparted on the samples. For every sample, > 110 psi was recorded, sufficient to ensure a flat, uniform sample, yet not sufficient to damage the crystal. Scans were collected from 4000 cm^{-1} - 400 cm^{-1}. Background scans were run prior to each sample. A total of 8 scans were collected per sample. Each sample was analyzed in replicate (n=5) to ensure reproducibility, and the automatic baseline correction tool was used on each spectrum. The five spectra were averaged for each sample, and the average spectrum was used in subsequent sample comparisons. The peaks were labeled using the software program using a threshold for peak detection of 1.00% transmittance. Along with the known samples, three blind samples (samples 12, 17, and 18) were also analyzed by FTIR-ATR to assess the discriminating ability of the technique.

3.3 MALDI-MS

A Voyager DE STR Biospectrometry Workstation with a MALDI-TOF Mass Spectrometer (Applied Biosystems, Foster City, CA) was used in this work. This instrument is located in the Mass Spectrometry Facility at Michigan State University.

Each of the 27 samples were prepared by extracting in ~0.1 mL dichloromethane (DCM), a solvent that dissolves many organic substances. Saturated solutions of each powder were prepared in DCM then filtered with an ultra-filter (0.2 μm) syringe to produce the sample solutions. A 0.5 μL aliquot of α-cyano-4-hydroxy-cinnamic acid matrix provided by the Mass Spectrometry Facility was placed in 34 separate wells of a 100-well stainless steel plate and allowed to dry. A 0.5 μL aliquot of each sample solution was placed in a particular well, and wells were also prepared containing DCM only (solvent blank), matrix only (matrix blank), a calibration standard containing the peptides bradykinin, angiotensin, and neurotensin (with masses of 1059.6, 1671.9, and 1295.7 amu respectively), and the three blind samples (samples 12, 17, 18).

The software provided a method to mass calibrate the instrument, a process that was done prior to collecting data. To calibrate the mass spectrometer, a mass spectrum of the calibration standard was first obtained. The reference file in the computer for the calibration standard being used was opened and compared to the mass spectrum obtained. The peaks in the initial mass spectrum were matched to the peaks in the reference spectrum with a mass tolerance of ±4 m/z. On matching peaks, the spectrum was saved and used as the calibration file for all samples.

The software program *Voyager Control Panel* (v. 5.1, Applied Biosystems, Foster City, CA) was utilized to set instrument parameters and to collect spectra, and the program *Data Explorer* 4.0 (Applied Biosystems) was used to visualize mass spectra. The instrument used a nitrogen laser (337 nm) and was operated in linear positive ion mode with 100 shots/spectrum and analyzed over an m/z range of 10-1000 amu. A spectrum was obtained for five different spots on each sample, and the five spectra were

averaged. The guide wire setting was at 0.05, and the delay time was 100 ns. The peak threshold for all the mass spectra was set at 0.1% of the intensity of the most abundant peak.

4. RESULTS AND DISCUSSION

4.1 SEM-EDS

The weight percentage of elements was calculated using Vontage 1.5.1 software (Noran Instruments). Calibration of the EDS is performed by the staff at the Center for Advanced Microscopy periodically using known metal standards. When determining values of atomic/weight percentages, a correction factor that contained atomic number effects (Z), absorption effects (A), and fluorescence effects (F), known as ZAF correction was applied in order to compensate for matrix effects and provide accurate quantitation.[6,17] These factors are described in detail below.

The two factors affecting characteristic x-ray emission that are dependent on atomic number are stopping power and backscattering.[26] Stopping power is the ability of the sample material to reduce the energy of an incident electron by inelastic scattering, which is related to the ratio of atomic mass number to the atomic number. The ratio increases with increasing atomic number.[26] The atomic number effect is the difference between the average atomic number of the sample and a calculated 100% pure standard. Therefore, if the mean atomic number of the standard differs from the sample, it must be accounted for in the Z correction.

The absorption factor occurs as a result of the neighboring atoms. If an atom emits an x-ray, the x-ray must pass through a certain distance within the sample. Within the distance traveled are surrounding atoms. These other atoms may absorb that energy, resulting in fewer x-rays observed in the spectrum.

Fluorescence occurs when the x-rays emitted from certain elements are absorbed by other elements, resulting in subsequent fluorescence. The ZAF correction factor compensates for all three of these effects.

During analysis, images of the powder samples were observed to be similar for all samples. Thus, morphology as a discrimination tool was not a useful means of classification. An EDS spectrum was collected for each of the samples (Figure 4.1.1). The tabulated atomic percentages for all samples were compared to distinguish samples based on elemental composition. The most common elements detected in the samples were oxygen (O), silicon (Si), aluminum (Al), magnesium (Mg), and iron (Fe). The high levels of O, Si, and Mg relative to other elements were not surprising as talc, a primary component of most face powders, has the chemical formula $Mg_{33}Si_4O_{10}(OH)_2$. Another possible source of the silicon was polydimethylsiloxane (PDMS), typically present in cosmetics as a skin softener and emollient.

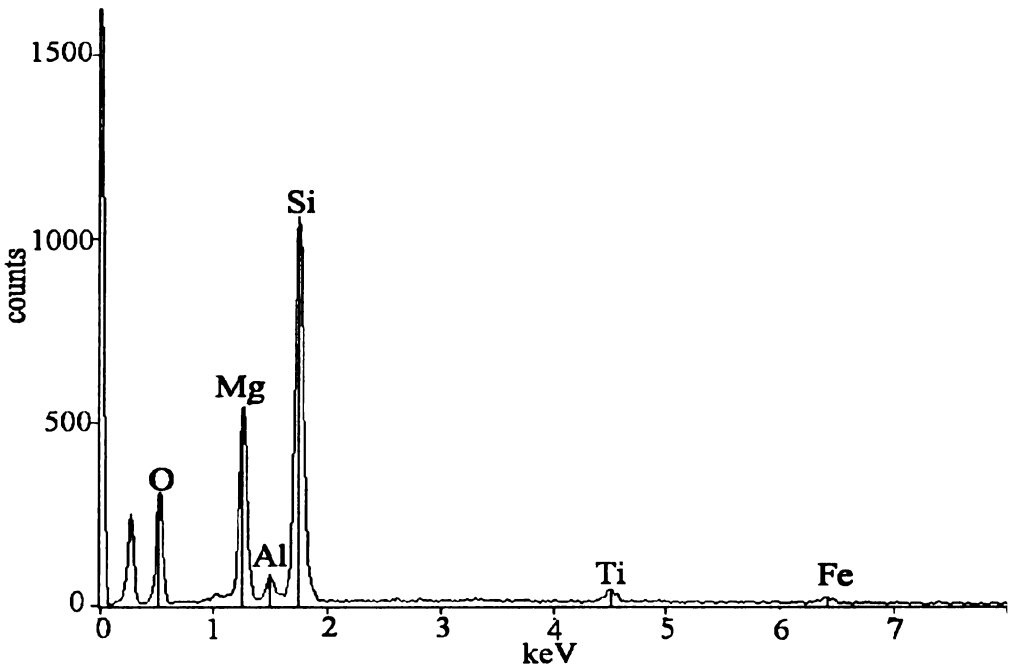

Figure 4.1.1. EDS spectrum of sample 6.

4.1.1 Sample Differentiation Based on Unique Elements

Along with these commonly found elements, there were also elements in some samples that were uncommon which allowed differentiation of these samples from the majority, as shown in Table 4.1.1. These elements included potassium (K), chlorine (Cl), sodium (Na), bismuth (Bi), titanium (Ti), fluorine (F), silver (Ag), zinc (Zn), and phosphorus (P) with weight percentages ranging from 1% to 8%. The major source of the fluorine in these samples is most likely Teflon®. Another possible contributor of fluorine is mica. Mica is a mineral sometimes found in cosmetics that contains F, and a period 1 element such as K, Na, or Ca, and either Al, Mg, or Fe.

Sodium could originate from common cosmetic ingredients such as sodium benzoate, or sodium laureth sulfate. Titanium dioxide, a white pigment, could account for the titanium in some samples. Zinc stearate, calcium carbonate, and iron oxides are also listed as possible ingredients for some samples.

The presence of these rare elements made several samples unique. For example, sample 3 was the only sample that did not contain oxygen, and it was also the only sample that contained silver. Samples 7 and 22 were the only ones that contained fluorine and could thus be distinguished from all other samples. The sixth ingredient listed on Sample 7 was PTFE, or Teflon®, while sample 22 had no ingredient list although is likely to also contain Teflon® or mica due to the presence of fluorine. Sodium was only found in samples 13 and 14, phosphorus was only present in sample 8, and zinc was found only in samples 3, 13, and 24. Samples 8 and 9 were the only powders containing calcium, while only sample 12 contained bismuth (Bi) and chlorine (Cl). However, no ingredient list was available for sample 12, so the ingredient that contributed these

elements is unknown. A possible ingredient containing both bismuth and chloride is bismuth oxychloride. This was listed under "may contain" on sample 15. However, the EDS spectrum of sample 15 did not contain either Bi or Cl, but since no product list label was located on sample 12, this ingredient could be a possible source of Bi and Cl in the spectrum of sample 12.

Table 4.1.1 Samples that could be identified based on unique characteristics

Sample number	Unique element(s)
3	no oxygen, silver, zinc
8	phosphorus, calcium
9	calcium
12	bismuth, chlorine
13	sodium, zinc
14	sodium
24	zinc
7 and 22	fluorine

While the presence of the less common elements could differentiate nine of the 27 samples (Table 4.1.1), the remaining 18 samples contained similar elements and hence could not be distinguished in a similar manner.

4.1.2 Sample Differentiation Based on Common Elements

All samples except for sample 3 contained O, Mg, Al, Si, and Fe at atomic percentages ranging from 1 to 66%. A hierarchical cluster analysis (HCA) was performed using the statistical software program, Minitab (version 14, Minitab, Inc., State College, PA) in an attempt to differentiate all samples based on differences in levels of O, Mg, Al, Si, and Fe present.

4.1.2.1 Cluster Analysis

Cluster analysis is a method for dividing a group of objects into classes so that similar objects are in the same class.[27] Samples are plotted in multi-dimensional sample

space and cluster analysis searches for objects which are close together in the variable space.[27] One of the most common distances used in cluster analysis is the Euclidian distance, *d*, that is computed from the sample data using equation 4.1.1:[27]

$$d = \sqrt{(x_1 - y_1)^2 + (x_2 - y_2)^2 + \cdots + (x_n - y_n)^2} \qquad \text{(eqn. 4.1.1)}$$

where x is a data set, y is a data set, and n is the number of data points in a set. When applying this to the SEM-EDS data, each face powder sample is a data set, and within each data set are six variables corresponding to the weight percentages of O, Mg, Al, Si, and Fe within that sample. The Euclidian distance can then be calculated between each sample data set. Once the distances between each of the samples are calculated, the data sets are clustered using the single linkage method which is based on the minimum distance between each cluster.[27] If two neighboring data sets are separated by a small Euclidian distance, they will most likely be clustered together. The similarity between samples is defined as:[27]

$$s = 100(1 - d_{xy} / d_{\max}) \qquad \text{(eqn. 4.1.2)}$$

where d_{xy} is the distance between two points, and d_{max} is the maximum separation between any two points.[27] The results of cluster analysis are often shown visually as a dendrogram, with similarity displayed on the y-axis and samples on the x-axis. Grouping of samples can be assessed at various levels of similarity; the higher the level of similarity, the more similar the samples are within that group.

The SEM-EDS data were inputted into the Minitab 14 software program; each sample was placed in a column, and six rows were present for each sample. Cluster analysis was performed using the Euclidean distance and single linkage method, and selecting a 90% similarity level. The resulting dendrogram was obtained (Figure 4.1.1):

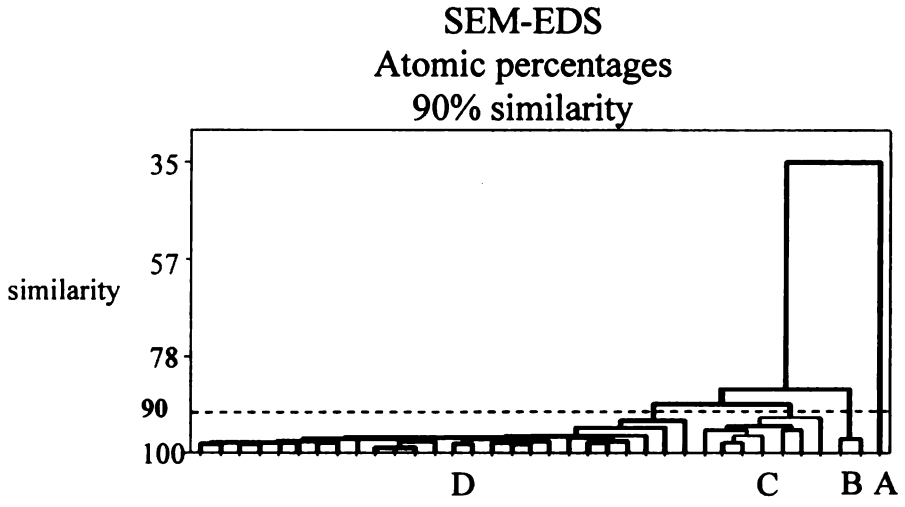

Figure 4.1.2 Resulting dendrogram from cluster analysis of atomic percentages at a similarity level of 90%. Tick marks on the x-axis correspond to each sample and each color represents a final clustering of samples.

At a similarity level of 90%, all samples (27) were divided into four clusters (A, B, C, and D) (Table 4.1.2). Cluster A contained only sample 3. It was expected that this sample would be in a separate group than the others, as it was the only sample that contained no oxygen as determined by SEM/EDS. It was therefore considered unique when looking at unique characteristics (Table 4.1.1). Cluster B contained sample 12 and one of the blind samples, which was also sample 12. Again, sample 12 was considered unique due to the presence of bismuth and chlorine. However, the blind sample 12 being clustered correctly with sample 12 provided further evidence of the accuracy of the technique. Cluster C contained samples 2a, 2c, 2d, and each of the triplicate samples for sample 2b. It was not surprising that 2a, 2b, 2c, and 2d were grouped together because the four samples were within the same compact, with similar ingredients listed for each, and were thus indistinguishable by SEM-EDS. However, within this cluster was also sample

14, but this was one of the samples previously determined unique based on the presence of sodium. It is unknown why sample 14 was grouped with samples 2, because no ingredient list was available for sample 14. The final cluster, cluster D, contained the remaining samples, which limited discrimination ability based on O, Si, Mg, Al, and Fe. These samples could not be distinguished from each other due to their large and similar amounts of O, Si, Mg, Al, and Fe. The presence of these major elements possibly masked the elements present at lower concentrations that may have been unique to such samples.

Table 4.1.2 Resulting clusters with 90% similarity

Cluster	Samples
A	3
B	12, 12 blind
C	2a, 2b, 2b, 2b, 2c, 2d, 14
D	4, 5, 6, 7, 8, 9, 10, 11, 13, 15, 16, 17, 18, 19, 20, 21, 21, 21, 22, 22, 22, 23, 24, 17 blind, 18 blind

It is important to note that for the three samples analyzed in triplicate, all were grouped within the same cluster, thus providing confidence in the reproducibility of SEM-EDS.

Based on the presence of unique elements and subsequent cluster analysis, 267 pairs out of 351 total pairs of samples could be distinguished, for a discrimination power of 76%. The discrimination power was limited by the large number of samples in cluster D, which could not be differentiated based on levels of O, Si, Mg, Al, and Fe.

4.2 FTIR Spectroscopy

IR spectra for each sample were compared visually, basing the comparison on the presence or absence of major peaks in the spectra. Many of the samples had peaks common with talc (Figure 4.2.1) which was expected because talc is a major component in face powders. A peak at ~3675 cm^{-1} was seen in all samples, and a trio of peaks at

2848, 2916, and 2957 cm^{-1} were seen in most samples. An exception to these common peaks was sample 12 which showed none of these, allowing differentiation of sample 12 from the remaining samples.

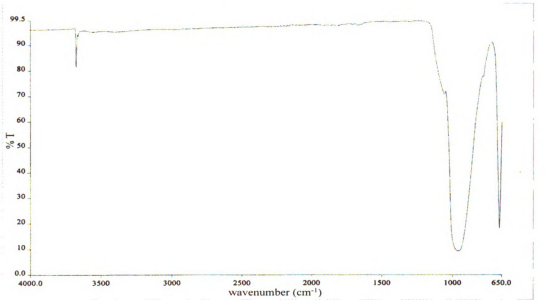

Figure 4.2.1 IR spectrum of talc

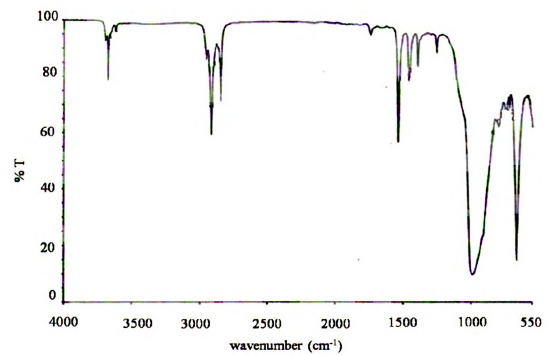

Figure 4.2.2 IR spectrum of sample 6

Although the samples shared many common peaks, there were a few prominent peaks that allowed classification of the samples into smaller groups. Samples were classed into two groups depending on the presence or absence of an absorbance at 1740 cm^{-1}, which is a characteristic carbonyl stretch found in aldehydes, ketones, carboxylic acids, or esters. Within each group, further classification was possible based on an absorbance at 1260 cm^{-1}, characteristic of a C-O stretch found in alcohols, ethers, carboxylic acids, or esters. The study by Gordon and Coulson also used peaks at ~1740 $cm^{-1}$and ~1640 cm^{-1} as discriminating characteristics for their foundation samples.[8]

Samples were further classified based on the presence or absence of peaks at 1538 cm^{-1} and 1638 cm^{-1}. The 1538 cm^{-1} peak is characteristic of the double bond in an aromatic ring, and the 1638 cm^{-1} peak is characteristic of a C=C in an alkene or C=O bond in an aldehyde, ketone, carboxylic acid, or ester.

The listed ingredients could account for several of the functional groups responsible for the peaks on the IR spectra. Stearic acid and palmitate, both compounds listed on several powders, contain a carboxylic acid. Allantoin, also a main ingredient contains several amide bonds. Parabens contain both an aromatic ring and ester bonds.

Using the four major peaks (1740, 1638, 1538, and 1260 cm^{-1}), a method for discrimination was developed to classify the samples. The classification scheme is shown in figure 4.2.1. By comparing the IR spectra visually, based on the presence or absence of these four major peaks, the 27 samples were classed into nine groups (Table 4.2.1).

Table 4.2.1 Nine groups based on presence or absence of major peaks (1740 cm^{-1}, 1260 cm^{-1}, 1538 cm^{-1}, and 1638 cm^{-1})

Groups	Sample
A	2a, 2b, 2c, 2d, 10, 21
B	9,11
C	16, 19
D	12, 14
E	13
F	3, 4, 5, 6
G	7, 22
H	15, 17, 18, 23, 24
I	1, 8, 20

It was possible to discriminate 313 pairs of samples out of a total 351 pairs, for a discrimination ability of 89%. In comparison, FTIR analysis of foundation samples by Gordon and Coulson yielded a discrimination ability of 98.3%.[8]

Figure 4.2.3. Classification of samples based on presence and absence of major peaks in IR spectra.

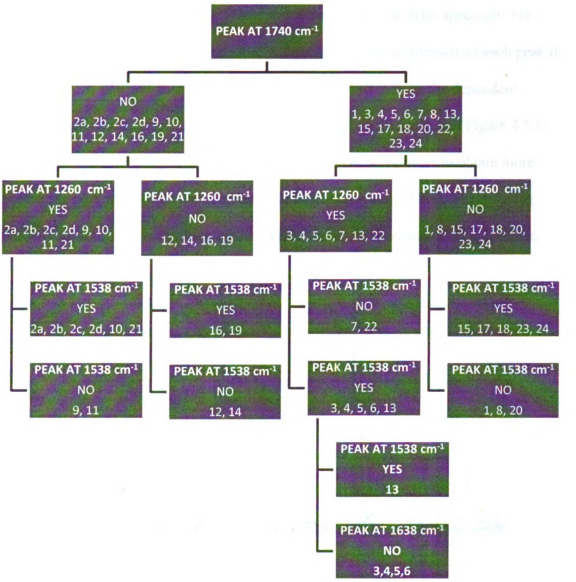

4.3 MALDI-MS

Mass spectral data for each sample were imported into a Microsoft Excel (Microsoft Corporation, Redmond, WA) spreadsheet to plot the mass spectrum. The spreadsheets had columns for the centroid mass and the relative intensity of each peak in the spectrum. A plot was then constructed with relative intensity as the dependent variable (y-axis), and centroid mass as the independent variable (x-axis) (Figure 4.3.1). Most of the peaks occurred at masses of less than 800 Da, so in order to obtain more detail in the plot, the x-axis was adjusted for a maximum value of 800. The resulting spectra were compared visually to assess similarities and differences among samples.

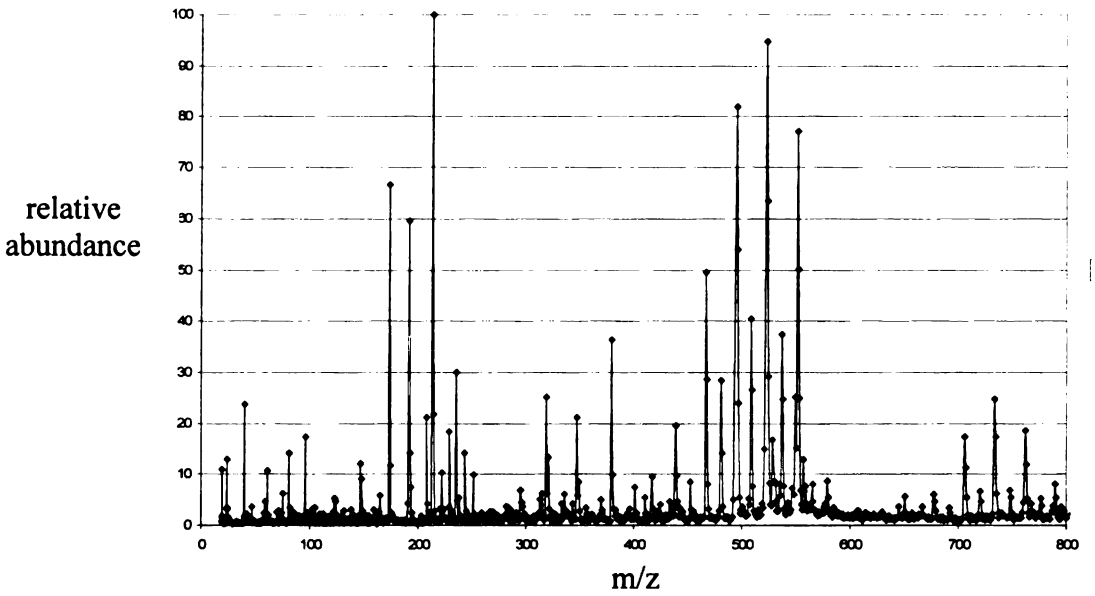

Figure 4.3.1 Mass spectrum of sample 13

When performing the experiment and preparing the samples on the MALDI plate, matrix solution was first pipeted onto each plate well followed by a small amount of sample. Due to this method, peaks on each mass spectrum could be attributed to the matrix. Therefore, when preparing the plate, there was a well reserved for matrix only,

and a well reserved for the extraction solvent (DCM) only, so a spectrum for each was obtained. The mass spectrum for each sample was first compared to the matrix spectrum, then the dichloromethane spectrum. Any peaks that were not present in the matrix or DCM spectra but were present in the sample spectra were recorded and used to compare samples.

There were three samples with obvious repeating patterns in their mass spectra. Sample 22 had peaks at m/z 440, 468, 496, and 524, as well as another pattern at m/z 662, 690, 718, 746, and 774. The difference in each of these groups is 28 mass units. In sample 7, this pattern of peaks with a difference of 28 mass units was also seen at m/z 690, 718, and 746. That pattern is also seen in sample 13 (m/z 705, 733, 761), and another pattern is seen with peaks separated by 14 mass units (m/z 467, 481, 495, 509, 523, 537, 551). The pattern of 14 and 28 mass unit differences is characteristic of fragmentation of an alkane chain, where 14 mass units represents a loss of $-CH_3$ and the addition of a proton, while 28 mass units represents a los of $-CH_2CH_3$ and the addition of a proton. Hence, the pattern of peaks observed in these samples corresponds to losses of methyl and ethyl groups with the simultaneous gain of a proton. However, since the actual masses are different, these groups are being lost from ions with a different molecular weight, and are thus different compounds.

These three samples (samples 22, 13, and 7) were classified into one group (Group A) that was different from all other samples because of the presence of these repeating patterns. However, further differentiation between the samples in Group A was possible. For example, sample 13 is different from both sample 7 and 22 because its pattern is in the 500 m/z range while the others' patterns are in the 400 and 700 m/z

range, respectively (Figure 4.2.3). This is most likely due to an alkane chain attached to different compounds or functional groups. Samples 7 and 22 could not be distinguished from one another based on this comparison.

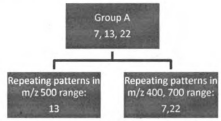

Group A = repeating patterns of 14 and 28 mass units

Figure 4.3.2. Scheme for differentiating powder samples in Group A based on MALDI-MS data

There were prominent peaks seen in the mass spectra of the remaining samples that would allow for further classification. The peak at m/z 615 was used as a characteristic to further classify the samples. This peak was observed only in the mass spectra of samples 9, 18, 23, 24, and the blind sample 18. Therefore, these were placed in Group B. Within this group, it was determined that these samples could be distinguished further. Sample 9 was the only one of the 5 samples in Group B that had a peak at m/z 538 but no peak at m/z 593. A peak at m/z 504 was present in samples 23 and 24, but not in 9 or 18. Sample 18 was different from the others in that it had no peak at m/z 538 or 504, yet did have a peak at m/z 504. Within group B, samples 9 and 18 were unique, and samples 23 and 24 could not be distinguished from each other (Figure 4.2.4). The m/z values discussed above could not be attributed to any of the ingredients listed on the products.

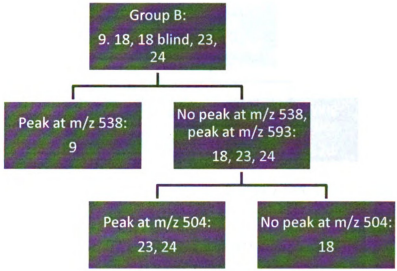

Group B = Mass spectra contains a peak at m/z 615

Figure 4.3.3. Scheme for differentiating powder samples in Group B based on MALDI-MS data

The remaining samples that were not already grouped into Group A or Group B were then examined, with a focus on whether or not a peak at m/z 538 was present, as it was one of the more intense peaks in the spectra. Spectra from samples 1, 2a, 2b, 2c, and 2d contained a peak at m/z 538. These were designated as belonging to Group C (Figure 4.2.5). Upon closer examination, sample 1 could be distinguished from the others from its peaks at m/z 328, 356, 494, 510, 522, and 550 that were not found in any of the powders from sample 2. However, samples 2a, 2b, 2c, and 2d could not be distinguished from each other, which was not surprising as they all came from the same compact.

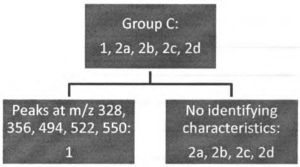

Group C = Peak at m/z 538

Figure 4.3.4. Scheme for differentiating powder samples in Group C based on MALDI-MS data

The remaining samples were placed into Group D. A summary of the initial groupings is outlined in table 4.3.1. However, these classifications were based on very obvious peaks observed in the spectrum.

Table 4.3.1 Initial grouping of MALDI-MS data

Group	Samples
A	7, 13, 22
B	9, 18, 23, 24, 18 blind
C	1, 2a, 2b, 2c, 2d
D	3, 4, 5, 6, 8, 10, 11, 12, 14, 15, 16, 17, 19, 20, 21, 12 blind, 17 blind

Group D had the most samples in it, and none had the high intensity peaks that were used to differentiate previous samples into groups (Figure 4.2.6). However, there were some small peaks (< 10% relative intensity) that were present that allowed further discrimination of the remaining samples.

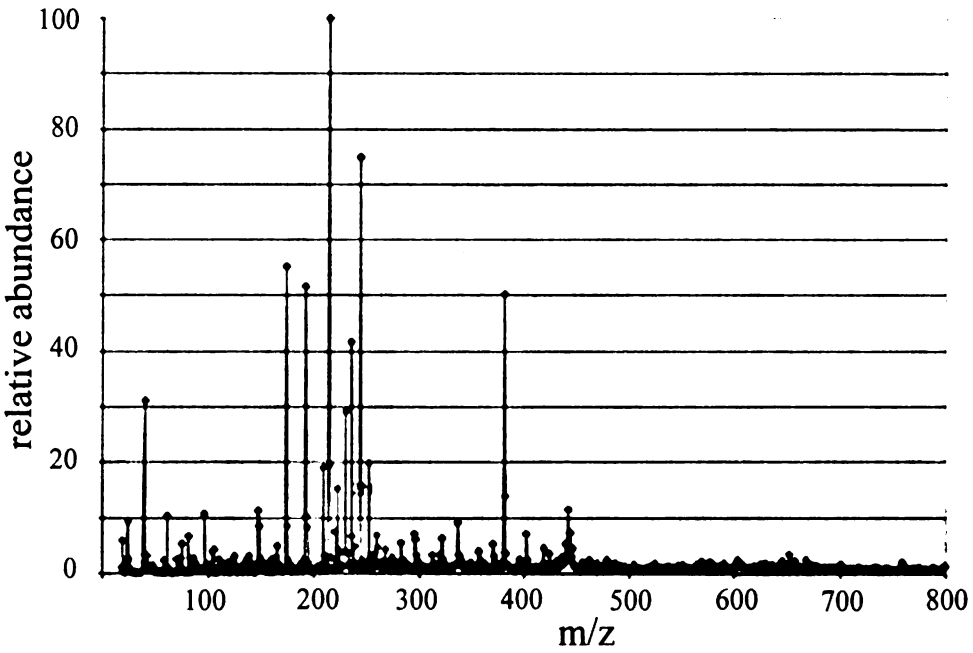

Figure 4.3.5. Mass spectrum of sample 6

Group D was broken down into two groups: Group D_i that included samples with a peak at m/z 320, and Group D_{ii} that included those samples with no peak at m/z 320 (Table 4.3.2).

Table 4.3.2 Initial classification of Group D based on presence of m/z 320

Group	Samples
D_i	3, 4, 5, 6, 10, 12, 12 blind
D_{ii}	8, 11, 14, 15, 16, 17, 19, 20, 21, 17 blind

Within Group D_i, samples 3 and 10 both had peaks at m/z 568 and 221 while the others did not. Also, sample 3 had a prominent peak at m/z 431 that all of the others did not have. Therefore, 3 and 10 could be distinguished from all other samples in Group D_i as well as each other. Sample 4 contained a peak at m/z 634 and samples 5 and 6 displayed a peak at m/z 282. Upon inspection of the spectra at m/z values greater than 800 Da, samples 4 and 12 (and blind sample 12) contained a peak at m/z 845 while 5 and 6 did not (Figure 4.2.7).

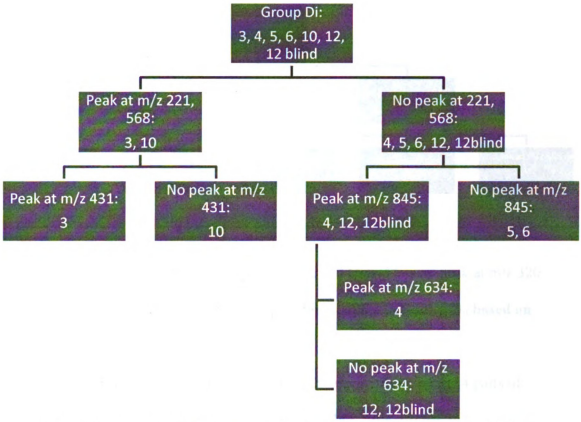

Group Di = does not fit into categories A, B, and C, and has peak at m/z 320.

Figure 4.3.6. Scheme for differentiating powder samples in Group D_i based on MALDI-MS data

Within Group D_{ii} further classification and identification could take place. For example, a peak at m/z 845 was seen in samples 11, 16, 17, 21, and blind sample 17, and within this subgroup 11 could be distinguished by a peak at m/z 551. Therefore, samples 16, 17, 21, and blind 17 could not be distinguished from each other. For those samples in Group D_{ii}, (samples 8, 14, 15, 19, and 20) with an absence of the 845 peak, an m/z 568 peak was characteristic of sample 15, and m/z 612 was characteristic of sample 8. Samples 14, 19, and 20 could not be distinguished from each other (Figure 4.2.8).

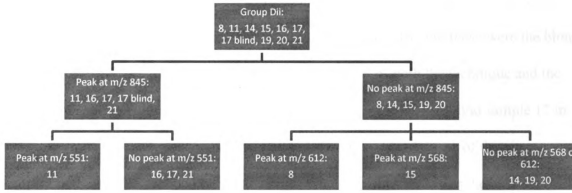

Group D_{ii} = does not fit into categories A, B, and C, and has no peak at m/z 320

Figure 4.3.7. Scheme for differentiating powder samples in Group D_{ii} based on MALDI-MS data

Using this classification of the MALDI-MS spectra, there were 14 pairs of samples that could not be distinguished from each other, for a discrimination ability of 96%.

4.4 Blind Samples

Prior to instrumental analysis, three samples were chosen at random to serve as blind samples. The samples selected were sample 12, 17, and 18, and these were the blind samples utilized for each technique to assess the accuracy of both the technique and the methods of sample comparisons. SEM-EDS classified sample 12 and blind sample 12 in the same group by cluster analysis. This particular sample was also one of the nine samples that could be grouped based on unique characteristics, as it was the only sample of the twenty seven that contained bismuth and chlorine. Both samples 17 and 18 could not be identified by unique characteristics. Based on the cluster analysis, samples 17 and 18 were grouped into group D, as were their corresponding blind samples. Using the FTIR method of discrimination based on the presence and absence of major peaks, each of the blind samples was grouped with their corresponding known sample. Both blind samples 17 and 18, and known samples 17 and 18 were also grouped with samples 15, 23, and 24. MALDI-MS also correctly classified each blind sample with its known sample. Sample 18 and blind sample 18 were uniquely identified, sample 12 and blind sample 12 were grouped with sample 4, and sample 17 and 17 blind were grouped with sample 16 and 21.

While the classification techniques based on SEM-EDS, FTIR, and MALDI-MS did not necessarily uniquely identify each sample, all of the blind samples were grouped correctly with their known counterparts. These classifications give further confidence to the discrimination abilities of each of the techniques.

4.5 Combined Techniques

Table 4.4.1 is a summary of the pairs of samples that could not be distinguished from each other using the three techniques individually. However, it is possible to combine the results of each technique to yield a higher discrimination ability than by using the individual results.

Table 4.4.1 Pairs of samples that could not be distinguished by SEM-EDS, ATR-FTIR, and MALDI-MS. Each row represents pairs that were indistinguishable by the technique in each column.

SEM-EDS	FTIR	MALDI-MS
2a, 2b, 2c, 2d	2a, 2b, 2c, 2d, 10, 21	2a, 2b, 2c, 2d
4, 5, 6, 10, 11, 15, 16, 17, 18, 19, 20, 21, 23	9, 11	5, 6
7, 22	16, 19	16, 17, 21
	3, 4, 5, 6	7, 22
	7, 22	14, 19, 20
	15, 17, 18, 23, 24	
	1, 8, 20	

For example, while samples 9 and 11 cannot be distinguished by FTIR, by using SEM-EDS and/or MALDI-MS they can be discriminated from each other based on elemental composition and mass spectra. Another example is samples 15 and 17 that can only be distinguished by their mass spectra, while their FTIR and SEM-EDS results could not be differentiated from each other. The final groupings of indistinguishable samples was different for each technique. This is because each technique examines different sample components and thus yields different information.

Together, SEM-EDS and FTIR could not distinguish between 18 pairs (333 out of 351, or 94.9% discrimination ability), SEM-EDS and MALDI-MS could not distinguish between 12 pairs (339 out of 351, or 96.9 % discrimination ability), and FTIR

combined with MALDI-MS could not distinguish between 8 pairs (343 out of 351, or a 97.7% discrimination ability).

There were some samples that could not be distinguished from each other by any of the methods used. Samples 7 and 22, while different from all other samples, were too similar to be distinguished from each other and were always grouped together by the three techniques. Sample 7 was Max Factor Colour Adapt face powder, while sample 22 was Covergirl TruBlend. Even though they were from different manufacturers, they most likely share a common major ingredient. Inspection of the labels provided no insight as to which ingredients because, on one of the samples (sample 22) no ingredients were listed. In addition, there were other Covergirl products that were analyzed and easily distinguished from sample 22; having the same manufacturer does not necessarily indicate that those samples could not be distinguished.

Each of the techniques was also unable to discriminate between samples 2a, 2b, 2c, and 2d. This was not completely unexpected, as these samples, while all separate samples, were in the same compact. There was a listing of ingredients, and also a list of ingredients that "may" have been contained in the powders. However, the list did not describe which ingredients were in which sample. It is possible that the ingredients that were listed were contained in each of the samples.

Samples 5 and 6 were the other pair that could not be differentiated. There was no manufacturer connection, as sample 5 was Loreal, and sample 6 was Covergirl, and a label containing the list of ingredients was not found on sample 6 for ingredient comparison.

Out of 351 total pairs of samples, SEM-EDS could distinguish 267 pairs (76% discrimination ability), FTIR could distinguish 313 pairs (89% discrimination ability), and MALDI-MS could distinguish 337 pairs (96% discrimination ability). The combined techniques can distinguish between 343 pairs. This is a discrimination ability of 97.7%.

5. CONCLUSIONS AND FUTURE RESEARCH

5.1 Conclusions

For cosmetic face powder samples, it is useful to determine whether two samples could have originated from the same source. Therefore, it was determined whether the techniques, SEM-EDS, FTIR, and MALDI-MS, could discriminate between pairs of samples. The three techniques can individually provide a high degree of discrimination when analyzing cosmetic face powders. However, because each technique provides different information regarding the samples of interest, when the three methods are combined, the resulting discrimination ability is high.

SEM-EDS provided elemental composition profiles of samples, and yielded the lowest discrimination ability, 76%. This was mainly a result of the common ingredient, talc, resulting in high atomic percentages of Mg, Si, and O. However, several samples contained more rare elements, for example bismuth, chlorine, or sodium that made these samples unique within the set.

A major issue of the SEM-EDS data in this work was that for each sample, only one spectrum was obtained. Ideally, at least three would be obtained and the resulting atomic percentages would be averaged. However, due to time constraints as well as cost, only one spectrum was generated, and therefore one atomic percentage value was determined for each element. However, triplicate spectra were obtained for three samples, all of which were reproducible. Blind samples were also analyzed and were correctly classified with the corresponding sample.

A method of determining similarity, cluster analysis, was performed on the EDS data for the samples. Each of the triplicate samples were grouped together. In addition,

the blind samples were all clustered within the same groups as their known counterparts. However at 90% similarity, only four groupings of the 27 samples were obtained.

Using ATR-FTIR, 89% of possible sample pairs were able to be distinguished. Many of the sample spectra had several peaks in common. However, a classification scheme based on the presence or absence of four major peaks allowed the samples to be grouped into nine groups. Each of these peaks was due to characteristic vibrations of functional groups within the samples. However, it was impossible from the IR spectra to determine which ingredient was responsible for IR absorption due to more than one possible ingredient containing the functional groups that vibrated at those particular frequencies. Based on the peaks at 1740, 1260, 1538, and 1638 cm^{-1} there were 313 pairs that could not be distinguished. The inability to distinguish between powders by FTIR was most like due to common, shared ingredients such as stearic acid, palmitate, or parabens which contain functional groups characteristic of the four peaks that were used for classification.

The final technique used was MALDI-MS, which resulted in a discrimination ability of 96%. MALDI is a powerful technique for elucidating structural information of samples. However, due to the complexity of samples, little information of the sample's molecular structure could be obtained, yet MALDI-MS provided a high degree of discrimination based on the presence or absence of major peaks in the mass spectra.

The MALDI technique requires the use of a matrix. The matrix itself contains numerous peaks in the resulting mass spectrum. This complicated visual analysis of the sample mass spectra. First, each sample spectrum had to be compared to the pure matrix spectrum , to discount any peaks in the sample that could be attributed to the matrix.

Most of the peaks found in the sample spectra were due to the matrix, leaving only a few that were useful for classification purposes. It would have simplified the process, and made it less time consuming, if it were possible for the software to subtract the matrix spectral peaks from the sample spectra.

Overall, the three analytical techniques provide powerful discrimination ability when analyzing cosmetic face powders, able to distinguish 343 out of 351 possible pairs of samples. The inability to distinguish some pairs was most likely the result of formulation similarities, as many samples shared common ingredients. There was no clear pattern of the inability to discriminate between certain pairs and their manufacturer. All of the sub-samples from sample 2 (2a, 2b, 2c, and 2d) were unable to be distinguished by all techniques. These samples were all in the same compact, and therefore from the same manufacturer, and had the same product ingredient lists. Sample 5 and 6, another pair that could not be distinguished by the combined techniques, were from different manufacturers, as were samples 7 and 22, another pair that could not be distinguished.

5.2 Future Research

As a preliminary study, this research has highlighted the potential of SEM/EDS, FTIR, and MALDI-MS for the discrimination of cosmetic face powders. However, before such techniques are commonly employed in crime laboratories, significant further research remains.

Cosmetics are prevalent in our society, and may therefore be encountered as forensic evidence at crime scenes. The ability to accurately determine type of powder, or to discriminate between powder samples can be useful in the field of forensic science. To date, little research has been performed dealing specifically with cosmetic face powders.

While this research provides some information regarding the ability of three techniques to discriminate between powder samples, there is much more that would prove beneficial in the analysis of cosmetic face powders.

Cosmetic face powder is applied over the entire facial region, and thus a large amount of transfer could occur. The transfer would most likely occur between skin and some type of substrate, most often clothing. Therefore, a useful experiment would be to apply the cosmetics to several different types of fabric, develop an extraction procedure to remove the powder from the clothing, followed by instrumental analysis. In addition, the interference effects of certain fabrics could be determined. Also, the existence of oils on skin would most likely have an effect on the results of the experiment. Obtaining wipings of powder directly from skin would be useful in ruling out interferences from naturally occurring skin excretions.

The mass spectra obtained in this work were extremely complex, making identification of compounds nearly impossible. Hence, it may be beneficial to employ a chromatographic technique to separate sample components prior to detection by MS. Identification of sample components based on fragmentation patterns in the mass spectra would be considerably simplified due to the initial separation of components. Another type of mass spectrometry such as GC-MS may be a more suitable method of analysis because MALDI-MS, while used extensively in research facilities, is not readily available in most forensic laboratories. GC-MS is routinely used in forensic analysis, however, extraction of face powder components would need to be performed before the sample could be injected into the instrument.

Another technique that would allow definitive identification of sample components is tandem MS, where each peak and its resulting fragmentation patterns are analyzed, making identification much simpler.

In this work, 27 samples were analyzed. However, on the market today there are several hundred kinds of face powders. Obviously, using a larger sample set would prove useful in determining the capability of these techniques to distinguish between samples. Due to cost of these types of products, the sample set was limited in number. In addition it may be useful to collect several powder samples from only one manufacturer to analyze and compare differences between the powders of one brand.

This research project was the first to examine the applicability of SEM-EDS, FTIR, and MALDI-MS to the analysis of face powders as forensic evidence. Overall, the three methods have shown to be complementary analytical techniques that provide a powerful means of discrimination among cosmetic face powder samples.

APPENDICES

APPENDIX A. Abbreviated Table of IR Group Frequencies for Organic Groups[16]

Bond	Type of Compound	Frequency Range (cm^{-1})
C—H	Alkane	2850-2970
C–H	Alkene	1340-1470
C–H	Alkyne	3010-3095
C–H	Aromatic rings	675-995
O–H	Monomeric alcohols, phenols	3590-3650
	hydrogen-bonded alcohols, phenols	3200-3600
	Monomeric carboxylic acids	3500-3650
	Hydrogen-bonded carboxylic acids	2500-2700
N–H	Amines, amides	3300-3500
C=C	Alkenes	1610-1680
C=C	Aromatic rings	1500-1600
C≡C	Alkynes	2100-2260
C–N	Amines, amides	1180-1360
C≡N	Nitriles	2210-2280
C—O	Alcohols, ethers, carboxylic acids, esters	1050-1300
C═O	Aldehydes, ketones, carboxylic acids, esters	1690-1760
NO_2	Nitro compounds	1500-1570 1300-1370

APPENDIX B. Listed ingredients in each sample

Sample	Ingredients contained in sample	Ingredients that may be contained
1	Not listed	
2a 2b 2c 2d	Talc, dimethicone, silica, zinc stearate, polyehylene, pentahydrosqualene, diisostearyl malate, lecitin, calcium silicate, nylon-12, retinyl palmitate, tocopheryl acetate, isopropyl isostearate, cyclomethicone, magnesuium ascorbyl phosphate, gingko biloba extract, panax ginseng root extract, camellia sinesis leaf (green tea), centaurea cyanus flower extract, vitis vinifera (grape) seed extract, alumina, calcium carbonate, conchiolin powder, pulverized rose quartz, pulverized topaz, polymethyl methacrylate, polyglycceryl-3 diisostearate, saccharomyces zinc ferment, saccharomyces copper ferment, saccharomyces manganese ferment, saccharomyces iron ferment, saccharomyces silicon ferment, saccharomyces potassium ferment, fragrance, diazolidnyl urea, ethylparaben, methylparaben, propylparaben	Mica, titanium dioxide, iron oxides, yellow 5, red 6, red 7, red 30, ultramarines, carmine
3	Salicylic acid	
4	None listed	
5	Talc, zea mays/corn starch, dimethicone, zinc stearate, pentaerthrityl tetraisostearate, octyldodecyl stearoyl stearate, zeolite, sorbic acid, methylparaben, propylparaben, tocopherylacetate, tetrasodim EDTA, butylparaben, BHT, panthenol	
6	None listed	
7	Talc, mica, ocyldodecyl stearoyl stearate, dimethicone, hydrogenated coco-glycerides, PTFE, methicone, lecithin, methylparaben, propylparaben, sodium dehydroacetate,	Titanium dioxide, iron oxides
8	None listed	
9	None listed	
10	None listed	
11	Talc, mica (and) titanium dioxide, hydroxyapatite, calcium carbonate, silica, dimethicone, methylparaben, butylparaben, mineral oil	Titanium dioxide, iron oxides, fragrence
12	None listed	
13	None listed	
14	None listed	

15	Talc, ethylhexyl palmitate, zinc stearate, caprilic/capric triglyceride, lauroyl lysine, magnesium myristate, methylparaben, sodium dehydroacetate, fragrance (parfum), prpylparaben, ascorbyl palmitate, glycine soja (soybean) oil, tocopherol, butylparaben, mica, iron oxides	Ultramarines, iron oxides, red 7 lake, carmine, bismuth oxychloride, manganese violet, titanium dioxide
16	None listed	
17	Talc, ethylhexyl palmitate, zinc stearate, juniperus communis (juniper) extract, aloe barbadensis extract, urtica dioica (nettle) extract, sambucus nigra (elder) flowers, propylene glycol, tocopherol, methylparaben, propylparaben, diazolidinyl urea, butylparaben ascorbyl palmitate	Titanium dioxide, iron oxides, ultramarines, mica
18	Talc, zinc stearate, octyldodecyl stearoyl stearate, mineral (paraffinum liquidum) oil, ethylhexyl palmitate, diazolidinyl urea, methylparaben, isostearyyl palmitate, aloe barbadensis leaf extract, propylparaben, allantoin, tocopheryl acetate, iron oxides	Titanium dioxide
19	None listed	
20	Synthetic wax, aluminum starch, octenylsuccinate, hydroxylated lanolin, isopropyl lanolate, petrolatum, cyclomethicone, cetyl acetate, acetylated lanolin alcohol, methylparaben, propylparaben	Mica, titanium dioxide, iron oxides, carmine, ultramarines, manganese violet, D&C Red No. 7, calcium latke, FD&C red No. 40, chromium oxide greens
21	None listed	
22	None listed	
23	Talc, zinc stearate, octyldodecyl stearoyl stearate, mineral (paraffinum liquidum) oil, ethylhexyl palmitate, diazolidinyl urea, methylparaben, isostearyyl palmitate, aloe barbadensis leaf extract, propylparaben, allantoin, tocopheryl acetate, iron oxides	Titanium dioxide
24	Talc, zinc stearate, octyldodecyl stearoyl stearate, mineral (paraffinum liquidum) oil, ethylhexyl palmitate, diazolidinyl urea, methylparaben, isostearyyl palmitate, aloe barbadensis leaf extract, propylparaben, allantoin, tocopheryl acetate, iron oxides	Titanium dioxide

REFERENCES

(1) http://www.cfsan.fda.gov/~dms/cos-toc.html.

(2) Stark, C. A. A Basic Study of Lipsticks Utilizing Microspectrophotometry, Laser Desorption/Ionization Mass Spectrometry, and Fourier Transform Infrared Spectroscopy, Michigan State University, 2005.

(3) Williams, D. F. a. S., W.H. *Chemistry and Technology of the Cosmetics and Toiletries Industry*; Chapman & Hall: London, 1992.

(4) http://www.azco.com/mica/micainfo.php.

(5) *International Journal of Toxicology* 2005, *24*, 65.

(6) Bilek, J. I. Forensic Analysis of Black Mascara via Microscopy, Fourier Transform Infrared Spectroscopy (FTIR), Scanning Electron Microscopy-Energy Dispersive Spectroscopy (SEM-EDS), and Visible Microspectrophotometry (MSP), Michigan State University, 2005.

(7) Choudhry, M. Y. *Journal of Forensic Sciences* 1991, *36*, 366.

(8) Gordon, A.; Coulson, S. *Journal of Forensic Sciences* 2004, *49*, 1244.

(9) Keagy, R. L. *Journal of Forensic Sciences* 1983, *28*, 623.

(10) Romero, L. A. A Protocol for the Analysis of Nail Polish, Michigan State University, 2003.

(11) Russell, L. W.; Welch, A. E. *Forensic Science International* 1984, *25*, 105.

(12) Ehara, Y. a. M., Y. *Forensic Science International* 1998, *96*, 1.

(13) Russell, L. W. a. W., A.E. *Forensic Science International* 1984, *25*, 105.

(14) Jasuja, O. P., and Singh, R. *Journal of Forensic Identification* 2005, *55*, 28.

(15) Rendle, D. F. *Chem. Soc. Rev.* 2005, *34*, 1021.

(16) Douglas A. Skoog, J. J. L. *Principles of Instrumental Analysis*, 4th ed.; Saunders College Publishing, 1992.

(17) Fleger, S. L., Heckman, John W. Jr., Klomparens, Karen L. *Scanning and Transmission Electron Microscopy An Introduction*; Oxford University Press: New York, 1993.

(18) www.chems.msu.edu/curr.stud/mse.sops/sem.det.htm.

(19) http://www.x-raymicroanalysis.com.

(20) James Ingle, S. C. *Spectrochemical Analysis*; Prentic Hall: New Jersey, 1988.

(21) Smith, A. L. *Applied Infrared Spectroscopy Fundamentals, Techniques, and Analytical Problem-solving*; John Wiley & Sons: New York, 1979.

(22) http://www.forensicmag.com/articles.asp?pid=95.

(23) Edmond de Hoffmann, V. S. *Mass Spectrometry Principles and Applications*, Second ed.; Wiley & Sons, Ltd.: England, 2002.

(24) www.asms.org.

(25) www.drnelson.utmem.edu.

(26) www.geo.ucalgary.ca.

(27) James Miller, J. M. *Statistics and Chemometrics for Analytical Chemistry*; Pearson Prentice Hall: England, 2000.